

# Muon spin rotation studies of electronic excitations and magnetism in the vortex cores of superconductors

J. E. Sonier\*

*Department of Physics, Simon Fraser University, Burnaby, British Columbia V5A 1S6, Canada*

The focus of this article is on recent progress in muon spin rotation ( $\mu$ SR) studies of the vortex cores in type-II superconductors. By comparison of  $\mu$ SR measurements of the vortex-core size in a variety of materials with results from techniques that directly probe electronic states, the effect of delocalized quasiparticles on the spatial variation of field in a lattice of interacting vortices has been determined for both single-band and multi-band superconductors. These studies demonstrate the remarkable accuracy of what some still consider an exotic technique. In recent years  $\mu$ SR has also been used to search for magnetism in and around the vortex cores of high-temperature superconductors. As a local probe  $\mu$ SR is specially suited for detecting static or quasistatic magnetism having short-range or random spatial correlations. As discussed in this review,  $\mu$ SR experiments support a generic phase diagram of competing superconducting and magnetic order parameters, characterized by a quantum phase transition to a state where the competing order is spatially non-uniform.

## INTRODUCTION

Muon spin rotation ( $\mu$ SR) is an experimental technique primarily used to measure local magnetic fields inside samples. The discovery of high-transition temperature (high- $T_c$ ) superconductivity in 1986 brought about a rapid world-wide expansion in the use and applications of  $\mu$ SR. Since then  $\mu$ SR has been routinely applied to investigations of these and other newly discovered type-II superconductors. The technique allows for studies in zero external magnetic field, which combined with its sensitivity as a local probe has provided distinctive information on the occurrence of internal magnetism as a co-existing or competing phase, or as a consequence of time-reversal symmetry breaking superconductivity. From zero-field  $\mu$ SR studies of cuprates, a generic temperature-vs-doping phase diagram has been constructed, showing the coexistence of high- $T_c$  superconductivity with static magnetism in lightly doped samples. Today there is still much debate on the origin of this magnetism and its importance to the high- $T_c$  ‘problem’.

The vortex state provides another avenue for investigation of type-II superconductors with  $\mu$ SR [1]. For many years such studies focussed solely on obtaining experimental information on the magnetic penetration depth ( $\lambda$ ), through measurements of the muon spin depolarization rate ( $\sigma$ ) resulting from the broad internal magnetic field distribution  $n(B)$  of the flux-line lattice (FLL). The temperature and magnetic field dependences of  $\lambda$ , which in many systems can also be determined in the Meissner phase by other techniques, reflect the pairing state symmetry of the superconducting carriers. With further advances of the  $\mu$ SR method came the ability to focus attention on the properties of the vortex cores themselves.

The first-ever study to account for the finite size of the vortex cores in the analysis of  $\mu$ SR data was an investigation by Herlach *et al.* [2] of  $n(B)$  in pure Nb single crystals. The measured field distributions were shown to

be consistent with numerical solutions of the microscopic BCS-Gor’kov theory. Some years later, the magnetic field dependence of the vortex core size was determined from  $\mu$ SR measurements on single-crystal NbSe<sub>2</sub> [3]. The results confirmed earlier scanning tunnelling spectroscopy (STS) measurements on NbSe<sub>2</sub> that showed a shrinking of the vortex cores with increasing magnetic field [4]. This behaviour could be attributed to an increased overlap of the quasiparticle states around a vortex core with those coming from neighbouring vortices. However, these  $\mu$ SR studies were more than just another means of accessing information obtainable by another experimental technique. Instead they marked the development of a more powerful method for investigating some of the intrinsic properties of vortex cores in type-II superconductors.

The STS technique, which is sensitive to the electronic structure of the vortex cores, is limited to probing individual vortices near the sample surface. Near the surface the vortices spread out [5, 6] and their properties are strongly influenced by surface inhomogeneities and/or defects. Today one can study vortices immediately above or below the surface by  $\mu$ SR using low-energy (several keV) positively charged muons ( $\mu^+$ ) [6, 7], or by  $\beta$ -detected NMR using low-energy radioactive ions [8]. In contrast, the experiments of Refs. [2, 3] used energetic ( $\sim 4$  MeV)  $\mu^+$  that stop at interstitial or bond sites in the bulk of the sample where they directly probe the local magnetic fields. The term “bulk” means that the stopping range of these faster muons is approximately 150 mg/cm<sup>2</sup>, which requires samples  $\sim 1$  mm thick. In further contrast to the STS method,  $\mu$ SR studies yield average information on the vortex cores, using  $\sim 10^7$   $\mu^+$  to randomly probe the  $\sim 10^9$  vortices in a typical size sample.

Since the experiments of Ref. [3], strong field and temperature dependences of the vortex-core size have been found by  $\mu$ SR in a variety of superconductors. Through comparison of the results with theoretical models and experiments that are directly sensitive to quasiparticles

properties, a good understanding of many of the  $\mu\text{SR}$  experiments has been achieved. In  $s$ -wave superconductors, it is now well established that the vortex core size depends on both the thermal occupancy of the bound quasiparticle core states and the overlap of the corresponding quasiparticle wave functions with those of nearest-neighbour vortices. However, in exotic systems such as high- $T_c$  superconductors, where localized cores states may be absent, there is currently insufficient experimental information to make similar definitive statements. On the other hand, recent  $\mu\text{SR}$  studies of the vortex cores in underdoped high- $T_c$  superconductors have shed new light on the ground state that emerges when superconductivity is suppressed. Combining information obtained from  $\mu\text{SR}$  experiments in zero and nonzero magnetic fields, the latest results support a picture of closely competing superconducting and magnetic ground states.

## MUON SPIN ROTATION ( $\mu\text{SR}$ )

### General description

The acronym  $\mu\text{SR}$  dates back to 1974, and stands for either ‘muon spin relaxation, rotation’ or ‘resonance’. These three terms describe different uses of the magnetic moment of a muon ( $\mu^-$  or  $\mu^+$ ) to probe matter. While the principle aspects of the technique are analogous to nuclear magnetic resonance (NMR), there are many important differences. Only some of these are touched upon in this review.

The primary use and strength of  $\mu\text{SR}$  is its unmatched sensitivity to internal magnetism. Central to the  $\mu\text{SR}$  method is the use of a nearly 100 % spin-polarized muon beam, naturally generated from the weak interaction decay of pions. This is a great advantage over conventional NMR, which relies on thermal equilibrium nuclear spin polarization in a large magnetic field. Zero-field (ZF)  $\mu\text{SR}$  is routinely used to study small internal magnetic fields of natural origin. In contrast to neutron scattering, the information provided by  $\mu\text{SR}$  is integrated over reciprocal space, which makes it ideal for studies of short-range magnetic correlations or disordered magnetism. The magnetic moment of the muon is 3.18 times larger than that of the proton, making it even more sensitive to magnetism than NMR. Although generally a nuisance in experiments,  $\mu\text{SR}$  even detects the dipolar fields of nuclear moments. In fact, magnetic fields as small as  $\sim 0.1$  G are detectable—although it is important to emphasize that this refers to the local field at the muon stopping *site*.

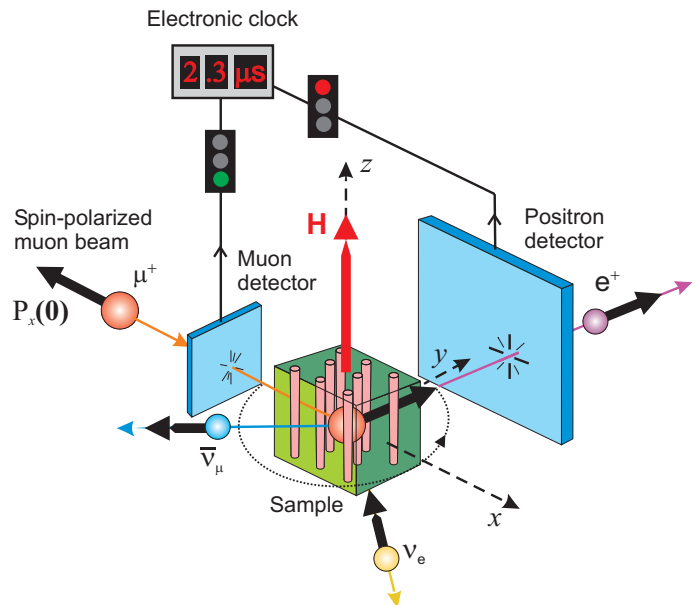


FIG. 1: Schematic of the arrangement for a TF- $\mu\text{SR}$  experiment on a type-II superconductor in the vortex state. The muon spin Larmor precesses about the local magnetic field  $B$  at its stopping site in the sample, and subsequently undergoes the three-body decay  $\mu^+ \rightarrow e^+ + \nu_e + \bar{\nu}_\mu$ . The time evolution of the muon spin polarization  $P_x(t)$  is accurately determined by detection of the decay positrons from  $\sim 10^6$  muons implanted one at a time.

### Transverse-field $\mu\text{SR}$

The internal magnetic field distribution  $n(B)$  of a type-II superconductor in the vortex state is measured by the so-called ‘transverse-field’ muon spin rotation (TF- $\mu\text{SR}$ ) method. The geometry of a TF- $\mu\text{SR}$  experiment is shown in figure 1. The external magnetic field  $H$  is applied *transverse* to the direction of the initial muon spin polarization  $P_x(0)$ , which defines the  $x$ -axis. In high- $T_c$  superconductors, the positive muon ( $\mu^+$ ) forms an  $\sim 1$  Å bond with an oxygen atom [9, 10], but in general the muon will stop at an interstitial site in the sample. There the muon spin precesses about the local magnetic field  $\mathbf{B}(\mathbf{r})$  in a plane perpendicular to the local field axis. The muon subsequently decays, emitting a fast positron. The angular dependence of the decay probability of the muon is given by

$$W(E, \theta) = 1 + a(E) \cos(\theta), \quad (1)$$

where  $E$  is the kinetic energy of the decay positron,  $\theta$  is the angle between the directions of the muon spin and the emitted positron, and  $a(E)$  is an asymmetry factor. When all positron energies are sampled with equal probability, the asymmetry factor has the value  $a=1/3$ . The statistical average direction of the muon spin polarization is obtained by measuring the anisotropic angular distribution of decay positrons from an ensemble of implanted

muons.

The  $\mu$ SR signal obtained by the detection of the decay positrons is given by

$$A(t) = a_0 P_x(t), \quad (2)$$

where  $A(t)$  is the  $\mu$ SR ‘asymmetry’ spectrum,  $a_0$  is the asymmetry maximum, and  $P_x(t)$  is the time evolution of the muon spin polarization

$$P_x(t) = \int_0^\infty n(B) \cos(\gamma_\mu B t + \phi) dB. \quad (3)$$

Here  $\gamma_\mu = 0.0852 \mu\text{s}^{-1} \text{G}^{-1}$  is the muon gyromagnetic ratio,  $\phi$  is a phase constant, and

$$n(B') = \langle \delta[B' - B(\mathbf{r})] \rangle, \quad (4)$$

is the probability of finding a local magnetic field  $B$  in the  $z$ -direction at a position  $\mathbf{r}$  in the  $x$ - $y$  plane.

### Application to studies of the vortex state

The internal magnetic field distribution  $n(B)$  measured by  $\mu$ SR is similar to what one can measure with NMR. However, because the muon has a spin equal to  $1/2$ , it does not possess an electric quadrupole moment and hence is a pure magnetic probe. In contrast,  $n(B)$  measured by NMR often includes quadrupolar broadening and in some cases closely spaced quadrupolar satellites. At its stopping site, a given muon *randomly* samples  $n(B)$ . This is because the intervortex spacing is typically several orders of magnitude larger than the atomic lattice spacing. For this reason it is often not necessary to know precisely where the muon stops in the sample.

Although the  $\mu$ SR signal is recorded in the time domain, a fairly accurate visual illustration of  $n(B)$  is provided by the Fourier transform of  $P(t)$ —often called the ‘ $\mu$ SR line shape’. An example of a  $\mu$ SR line shape for  $\text{YBa}_2\text{Cu}_3\text{O}_{6.95}$  is shown in figure 2. Included in this figure is  $n(B)$  of equation (3) obtained from a fit to the asymmetry spectrum, the details of which are described later in this article. Despite the Gaussian apodization used in generating the Fourier transform, the  $\mu$ SR line shape closely resembles  $n(B)$  obtained from the fit to the  $\mu$ SR signal in the time domain. Note that  $n(B)$  differs somewhat from that expected for an ideal FLL, because of FLL disorder and the contribution from nuclear dipoles.

As shown in figure 3, the minimum size of the sample required for  $\mu$ SR studies has greatly decreased over the years. Today’s capability to probe smaller samples comes from several key developments. Like neutron scattering, the quality of  $\mu$ SR spectra are limited by counting times and background contributions. Shorter data collection times and smaller background signals have been achieved

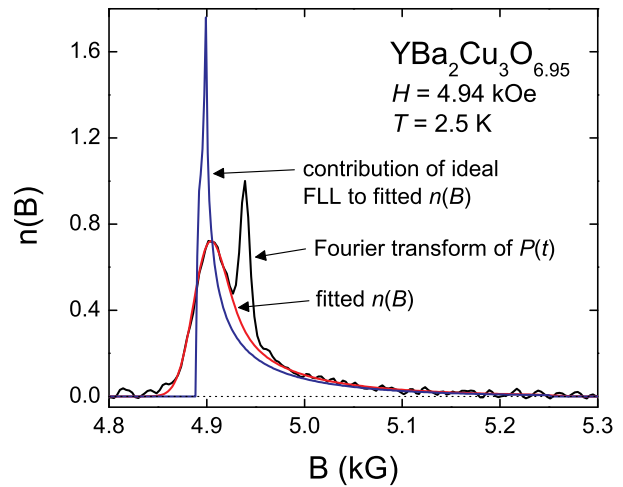


FIG. 2: Fourier transform of the TF- $\mu$ SR signal from single crystal  $\text{YBa}_2\text{Cu}_3\text{O}_{6.95}$  at  $T = 2.5 \text{ K}$  and  $H = 4.94 \text{ kOe}$  (black curve) computed using a Gaussian apodization function with a width of  $3 \mu\text{s}^{-1}$ . The peak at  $B \approx 4.94 \text{ kG}$  is a background signal coming from muons stopping outside the sample. Also shown is the internal magnetic field distribution  $n(B)$  (red curve) obtained from fits to the  $\mu$ SR precession signal. The fit assumes  $n(B)$  of an ideal FLL (blue curve) generated from a Ginzburg-Landau model described later, and additional broadening by FLL disorder and nuclear dipole moments.

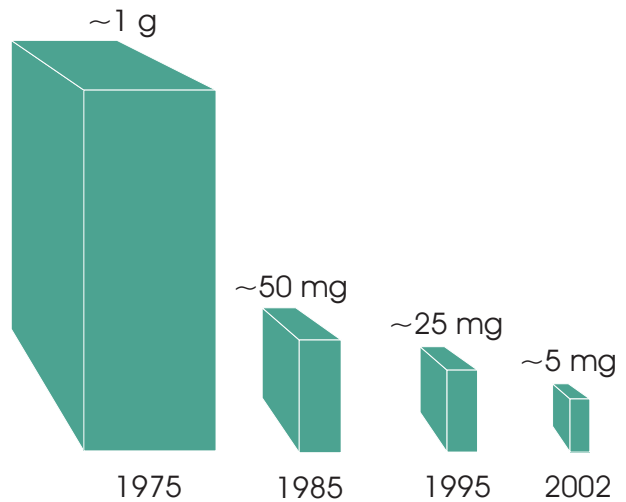


FIG. 3: Evolution of the minimum sample size required for  $\mu$ SR studies of the vortex state.

through the availability of higher luminosity muon beam lines, which allow more of the beam to be focused on the sample. Major advancements in  $\mu$ SR spectrometer design [11, 12] have also greatly helped in suppressing the background signal arising from muons that miss the sample and stop elsewhere. In many setups this is achieved by placement of the muon and positron counters within the same cryogenic environment as the sample. This

tighter geometry makes it easier to restrict the *good* decay events to those associated with muons stopping in the sample. The background peak that contributes to the  $\mu$ SR line shape in figure 2 constitutes  $\sim 12\%$  of the total signal, and is accounted for by adding a polarization function  $\exp(-\sigma_{\text{bg}}^2 t^2/2) \cos(\gamma_\mu B_{\text{bg}} t + \phi_{\text{bg}})$  with 12% amplitude to equation (3). This  $\mu$ SR line shape was recorded in 1992. As shown later, today this same measurement can be done with virtually no background signal. However, it is often helpful in the analysis of such data to have some background, as it provides an accurate determination of the average magnetic field at the sample position.

### THE MUON DEPOLARIZATION RATE

In the London model the local magnetic field for a perfect FLL is

$$B(\mathbf{r}) = B_0 \sum_{\mathbf{G}} \frac{e^{-i\mathbf{G}\cdot\mathbf{r}}}{1 + \lambda^2 G^2}, \quad (5)$$

where the sum is over reciprocal lattice vectors  $\mathbf{G}$  of the FLL. This equation is considered valid provided  $\lambda \gg \xi$  and  $B \ll B_{c2}$ , where  $\xi$  is the superconducting coherence length and  $B_{c2}$  is the upper critical field. The second moment of the internal magnetic field distribution  $n(B)$  corresponding to equation (5) is [13]

$$\langle(\Delta B)^2\rangle = \langle(B(\mathbf{r}) - \langle B \rangle)^2\rangle = \eta \Phi_0^2 \lambda^{-4}, \quad (6)$$

where  $\langle B \rangle$  is the average of  $n(B)$ ,  $\Phi_0 = hc/2e = 2.07 \times 10^{-15}$  T-m<sup>2</sup>, and  $\eta = 0.00371$  and  $\eta = 0.003868$  for a hexagonal and square FLL, respectively [14]. In the London model  $\langle(\Delta B)^2\rangle$  is independent of the applied field. In high- $T_c$  superconductors, where the effective mass of the charge carriers is larger in the direction perpendicular to the  $\text{CuO}_2$  layers compared to that parallel to the  $\text{CuO}_2$  layers,  $\lambda$  is highly anisotropic. If the field is applied along the  $\hat{c}$ -axis, then  $\lambda = (\lambda_a \lambda_b)^{1/2} \equiv \lambda_{ab}$ , where  $\lambda_{ab}$  is the in-plane magnetic penetration depth describing screening currents flowing in the  $\hat{a}$ - $\hat{b}$  plane around a vortex. Applying the field perpendicular to the  $\hat{c}$ -axis results in the formation of Josephson vortices sandwiched between  $\text{CuO}_2$  layers. In this case the screening currents flow in the  $\hat{a}$ - $\hat{c}$  or  $\hat{b}$ - $\hat{c}$  plane, and  $\lambda = (\lambda_a \lambda_c)^{1/2} \equiv \lambda_{ac}$  or  $\lambda = (\lambda_b \lambda_c)^{1/2} \equiv \lambda_{bc}$ , respectively. The out-of-plane penetration depth  $\lambda_c$  is typically much greater than 5000 Å, so that  $\langle(\Delta B)^2\rangle$  is significantly reduced in this geometry. For such large values of the magnetic penetration depth, the width of the  $\mu$ SR line shape in the vortex state becomes comparable to that in the normal state, and this prevents an accurate determination of the temperature dependence of  $\lambda$ . The absolute values of  $\lambda_a$ ,  $\lambda_b$  and  $\lambda_c$  cannot be isolated by  $\mu$ SR without a priori knowledge of the mass anisotropies. For example, if it is

known that  $\lambda_b = \lambda_a$ , then  $\lambda_a$  can be determined from a measurement of  $\lambda_{ab}$ , and  $\lambda_c$  can be determined from a subsequent measurement of  $\lambda_{ac}$ . This has been done for the heavy-fermion superconductor  $\text{UPt}_3$  [15].

For polycrystalline samples an often used approximation is to assume  $n(B)$  is a simple Gaussian distribution of fields of width  $\sigma$

$$n(B) = \frac{\gamma_\mu}{\sqrt{2\pi}\sigma} \exp\left(-\frac{1}{2} \frac{\gamma_\mu^2 B^2}{\sigma^2}\right), \quad (7)$$

in which case equation (3) has the following form

$$P_x(t) = \exp(-\sigma^2 t^2/2) \cos(\gamma_\mu \langle B \rangle t + \phi). \quad (8)$$

The width  $\sigma$  is thus equivalent to the damping rate of the asymmetry spectrum, called the ‘muon depolarization rate’. There is generally a temperature-independent contribution to  $\sigma$  from randomly oriented nuclear dipole fields, which can easily be determined from measurements above  $T_c$ . The resultant measured value of  $\sigma$  can then be used to obtain the second moment of the Gaussian distribution  $n(B)$

$$\langle(\Delta B)^2\rangle = \sigma^2/\gamma_\mu^2. \quad (9)$$

By equating equation (6) to equation (9), one gets an estimate of  $\lambda$

$$\sigma = \eta \gamma_\mu \Phi_0 \lambda^{-2}. \quad (10)$$

For large anisotropy  $\gamma \equiv (m_c/m_{ab})^{1/2} = \lambda_c/\lambda_{ab} > 5$  the effective penetration depth  $\lambda$  is primarily determined by  $\lambda_{ab}$ , such that

$$\lambda \simeq f \lambda_{ab}, \quad (11)$$

where  $f = 1.23$  [16]. For  $\gamma = 1$  to 5,  $f$  varies from 1 to 1.23.

Early  $\mu$ SR measurements of  $\sigma$  were used to deduce information about  $1/\lambda_{ab}^2$  using equations (10) and (11). From observations of a weak temperature dependence for  $\sigma$  at low  $T$  it was concluded that the pairing state symmetry of high- $T_c$  superconductors is *s*-wave [17, 18, 19, 20]. A linear scaling of  $T_c$  with  $\sigma$  was also found (the so-called ‘Uemura plot’), which has been interpreted via equation (10) to imply  $T_c \propto 1/\lambda_{ab}^2$ , which in turn is proportional to the superfluid density  $n_s$  [21, 22]. While the dependences of  $\sigma$  for newly discovered superconductors continue to be reported in the literature, the assumed relation  $\sigma \propto 1/\lambda_{ab}^2$  is not precisely correct. One reason is that the use of equation (10) assumes one is aware of and understands all contributions to the measured value of  $\sigma$ . Brandt [13] has shown that for straight rigid vortex lines,  $\sigma$  is increased by both pinning-induced random displacements of the vortices from their ideal position in the FLL and thermal fluctuations of the vortex lines. On the other hand, the layered nature of the high- $T_c$  superconductors

means that the vortices can be highly flexible. In this case segments of a flux line are susceptible to pinning or thermal-induced displacements, which reduce  $\sigma$ . In either situation the size of the effect will be dependent on temperature and the applied magnetic field. There may also be contributions to  $\sigma$  from static electronic moments. This is likely to be the case in rare-earth and lightly-doped cuprate superconductors. Even if identified, these contributions to  $\sigma$  cannot be reliably separated from the depolarization rate associated with  $\lambda_{ab}$ .

A second consideration is that Yaouanc, Dalmas de Réotier and Brandt [23] have shown that the second moment due to an ideal hexagonal FLL is more accurately given by

$$\langle(\Delta B)^2\rangle = 0.00371\Phi_0^2\lambda^{-4}f_v(b), \quad (12)$$

where  $b = B/B_{c2}$  is the reduced field and  $f_v(b)$  is a universal function that accounts for the finite size of the vortex cores. It is often assumed that the vortex cores of high- $T_c$  superconductors are small (*i.e.*  $\xi_{ab} \approx 15 \text{ \AA}$ ), so that little error is introduced in neglecting them. However, measurements by other techniques indicate that the vortex core radius can greatly exceed  $15 \text{ \AA}$  in underdoped and overdoped samples [24, 25, 26]. As explained in Refs. [23, 27],  $f_v$  is strongly dependent on  $b$ . Moreover, Brandt [27] has shown that the often used approximation  $f_v = 1$  is really only satisfactory over a narrow field range and only for  $\kappa \geq 70$ . The latter condition is not always satisfied in high- $T_c$  superconductors.

A third problem is the assumption that  $n(B)$  is a Gaussian distribution. In a polycrystalline sample  $n(B)$  is an average over all orientations [13, 28]. An example of what  $n(B)$  should look like in an unoriented powder sample is shown in figure 4. The fact that many of the early  $\mu$ SR line shapes from measurements on polycrystalline samples of high- $T_c$  superconductors looked Gaussian-like, suggests that the samples were of poor quality with a high-degree of FLL disorder.

Given these issues, the dependences of  $\sigma$  should be viewed as providing the correct qualitative trends of  $1/\lambda^2$  only. Indeed the Uemura plot was an important achievement, as it established for the first time a qualitative relationship between  $T_c$  and the superfluid density. However, the current state of affairs regarding the search for a microscopic theory of high- $T_c$  superconductivity is such that precise quantitative relations are desired. In recent years, experimental studies of  $1/\lambda^2$  have shown that  $T_c$  is a sublinear function of  $n_s$  in the underdoped regime [29, 30, 31] and that there is no single universal Uemura relation for high- $T_c$  cuprates [32]. Likewise, experiments on single crystals [33], including  $\mu$ SR [34, 35], have established a limiting low-temperature linear  $T$  dependence of  $\lambda_{ab}$ , that is not evident in the earlier measurements of  $\sigma$ . This behaviour is consistent with a  $d_{x^2-y^2}$ -wave superconducting order parameter, which has been clearly identified by phase-sensitive techniques [36].

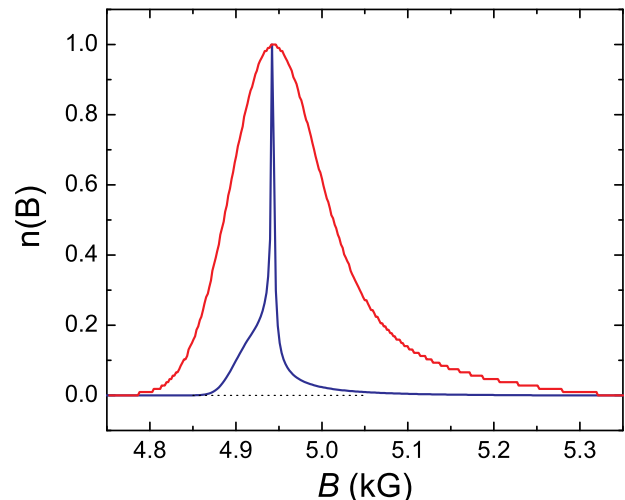


FIG. 4: Theoretical field distributions for an *unoriented polycrystalline* sample calculated from the ‘Kossler model’ for the powder average of an anisotropic superconductor [28] and including FLL disorder. The parameters used to generate the blue curve come from the fit of *single crystal*  $\text{YBa}_2\text{Cu}_3\text{O}_{6.95}$  in figure 2. The red curve is calculated with a higher degree of FLL disorder (*i.e.*  $\sigma_d$  of equation (15) is three times larger), and is closer to a Gaussian distribution. (Note that the two curves for  $n(B)$  are not normalized with respect to each other.)

## FULL LINE SHAPE ANALYSIS

To extract values of  $\lambda$  and the vortex core size from TF- $\mu$ SR measurements, one must assume a model for the internal magnetic field distribution  $n(B)$ . This in fact is the largest source of uncertainty in these kinds of measurements. To date, the analysis of  $\mu$ SR measurements in the vortex state have primarily relied on models based on either the phenomenological London or Ginzburg-Landau (GL) theories. The reason is that in some limiting cases, analytical models for the spatial field profile  $B(\mathbf{r})$  exist for these theories. While the analytical London and GL models provide very good fits to  $\mu$ SR measurements of the FLL in real materials, neither are generally valid, and considerable effort has been devoted in recent years to understanding the meaning of the fitted parameters  $\lambda$  and  $\xi$ . In particular, it is important to consider the following cautionary statements, which are discussed in further detail in the following sections:

- Generally speaking, **the fitted parameter  $\lambda$  is not a measure of the magnetic penetration depth**. This is because  $\lambda$  is influenced by deviations of the assumed theoretical model for  $n(B)$  from the actual field distribution of the FLL in the sample. This point was made in Refs. [23, 37, 38, 39, 40, 41, 42, 43, 44, 45]. For this reason, the magnetic penetration depth actually corresponds to the

extrapolated  $H \rightarrow 0$  value of  $\lambda$ .

- Likewise, **the fitted parameter  $\xi$  is generally not a measure of the superconducting coherence length.** This point is explained in detail in Ref. [40]. Instead  $\xi$  qualitatively tracks changes in the vortex core size that have nothing to do with the size of the Cooper pairs.

On the theoretical front, great strides have been made in numerically calculating  $n(B)$  from the microscopic equations. The predictions of the microscopic theory provide one means of determining the accuracy of the phenomenological approach to modelling  $\mu$ SR measurements.

### Finite core size

#### *Modified London models.*

The London model does not account for the spatial dependence of the superconducting order parameter and consequently equation (5) breaks down at distances on the order of  $\xi$  from the vortex core centre—*i.e.*  $B(r)$  diverges as  $r \rightarrow 0$ . To correct this, the  $\mathbf{G}$  sum can be truncated by multiplying each term in equation (5) by a cutoff function  $F(G)$ . It is important to stress that the appropriate form of  $F(G)$  depends on the precise spatial dependence of the order parameter in the vortex core region, and this in general depends on temperature and magnetic field.

Analytical expressions for  $F(G)$  exist only for certain limiting cases. Some time ago Brandt suggested the use of a smooth Gaussian cutoff factor

$$F(G) = \exp(-\alpha G^2 \xi^2). \quad (13)$$

If there is no dependence of the superconducting coherence length  $\xi$  on temperature and magnetic field, then changes in the spatial dependence of the order parameter around a vortex correspond to changes in  $\alpha$ . By solving the GL equations, Brandt determined that  $\alpha = 1/2$  at fields near  $B_{c2}$  [13, 46, 47], and arbitrarily determined that  $\alpha \approx 2$  at fields immediately above  $B_{c1}$  [48]. More accurate values of  $\alpha$  have since been obtained from precision solutions of the GL equations. For an isolated vortex in an isotropic extreme ( $\kappa \gg 1$ )  $s$ -wave superconductor,  $\alpha$  is found to decrease smoothly from  $\alpha = 1$  at  $B_{c1}$  to  $\alpha \approx 0.2$  at  $B_{c2}$  [49]. Even so, it is rather presumptuous to incorporate the field dependence of  $\alpha$  into the analysis of  $\mu$ SR spectra, as the vortices in real materials are not isolated. Furthermore, the additional effects of temperature on the spatial dependence of the order parameter in the vortex core region are not accounted for in calculations of  $\alpha(B)$ . For example, Laiho *et al.* [43, 50] have shown by comparison to solutions of the quasiclassical Eilenberger equations for a  $d_{x^2-y^2}$ -wave superconductor that

$\alpha$  is temperature dependent. More recently they have determined the magnetic and temperature dependences of the cutoff function used in the London model by numerically solving the quasiclassical Eilenberger equations for the vortex state of an  $s$ -wave superconductor [44]. These calculations show that the London model with the proper cutoff function provides a reasonable description of the field distribution of the FLL in real superconductors.

Generally,  $\alpha$  is fixed when using the modified London model to fit  $\mu$ SR spectra, so that the temperature and magnetic field dependences of the order parameter are indicated by variations in the fitted value of  $\xi$ . Such a procedure has been used to account for the finite size of the vortex cores in a number of  $\mu$ SR studies of the vortex state in type-II superconductors [34, 51, 52, 53, 54, 55]. Unfortunately, none of these studies were done at sufficiently low enough temperature to make a direct comparison of the field dependence of  $\xi$  with the theoretical predictions for  $\alpha(B)$  at  $T = 0$  K.

#### *Ginzburg-Landau models.*

In recent years, modified London models for  $B(\mathbf{r})$  have been abandoned by some in favour of models based on GL theory. The appealing aspect of the GL models is that the spatial variation of the order parameter is naturally built into the theory. The drawback is that GL theory assumes that the order parameter varies slowly in space and is strictly valid only near  $T_c$ . Despite these limitations, GL theory has proven to be highly successful in describing variations of  $n(B)$  as measured by  $\mu$ SR, yielding accurate quantitative values of  $\lambda$  and  $\xi$  in certain cases. As is the case in using modified London models, the key is to be careful with the interpretation of the fitted values.

The GL equations for the ideal Abrikosov vortex lattice can be solved by a variational method [56]. At low reduced fields  $b = B/B_{c2} \ll 1$  and for  $\kappa \gg 1$ , an excellent analytical approximation to the spatial field profile in GL theory is [23]

$$B(\mathbf{r}) = B_0(1 - b^4) \sum_{\mathbf{G}} \frac{e^{-i\mathbf{G}\cdot\mathbf{r}} F(G)}{\lambda^2 G^2}, \quad (14)$$

where  $F(G) = u K_1(u)$ ,  $u^2 = 2\xi^2 G^2 (1 + b^4) [1 - 2b(1 - b)^2]$ , and  $K_1(u)$  is a modified Bessel function. Note the cutoff function  $F(G)$  depends on the local internal magnetic field  $B$ .

Brandt later introduced an iterative procedure for solving the GL equations for arbitrary  $b$ ,  $\kappa$  and vortex-lattice symmetry [57]. While more generally applicable, fitting  $\mu$ SR spectra with this iterative method requires a tremendous amount of computer time. Fortunately, it does not seem that this is necessary. In a recent  $\mu$ SR study of the low- $\kappa$  type-II superconductor V, qualitatively similar results were obtained from analyses with

the variational and iterative solutions of the GL equations [42].

#### *Vortex symmetry.*

In the above models the individual vortices are assumed to have circular symmetry. However, this is not the case in real type-II superconductors with anisotropic Fermi surfaces and/or superconducting energy gaps [58, 59, 60, 61, 62]. At magnetic fields where there is an appreciable degree of overlap of the vortices, the FLL adopts the symmetry of the individual flux lines. In cases where the deviation from circular symmetry is extreme, the symmetry of the FLL can be accounted for in the model for  $B(\mathbf{r})$ . This has been successfully done in  $\mu$ SR studies of  $\text{YNi}_2\text{B}_2\text{C}$  [54],  $\text{LuNi}_2\text{B}_2\text{C}$  [55],  $\text{Sr}_2\text{RuO}_4$  [63],  $\text{V}_3\text{Si}$  [64] and  $\text{Nb}_3\text{Sn}$  [65]. In the case of  $\text{V}_3\text{Si}$ , it was possible to extract from the  $\mu$ SR measurements a gradual hexagonal-to-square transformation of the FLL symmetry in good agreement with STS imaging experiments. A couple of measurements from this study are shown in figure 5.

In Refs. [54, 55, 64], the theoretical models used for analysis of the TF- $\mu$ SR spectra are based on London theory [60, 61]. London models that account for the fourfold symmetry of the  $d_{x^2-y^2}$ -wave order parameter in cuprate superconductors have also been developed [37, 66]. Anisotropy may also be incorporated into analytical GL models. The TF- $\mu$ SR study of  $\text{Sr}_2\text{RuO}_4$  [63] employed a GL model that accounts for  $p$ -wave symmetry and Fermi surface anisotropy [67, 68]. Since all of the theoretical models accounting for anisotropy introduce additional fitting parameters, they are seldom used in  $\mu$ SR studies. When anisotropy is not included in the model for  $B(\mathbf{r})$ , the fitted values of  $\lambda$  and  $\xi$  are angle-averaged length scales.

### **Vortex Lattice Disorder**

#### *3D vortex lines.*

The effects of random pinning and thermal fluctuations of the vortices on  $n(B)$  depend very much on the rigidity of the vortex lines. In general, reliable information on the length scales  $\lambda$  and  $\xi$  is obtained only when the vortices are fairly straight and parallel. In this case, pinning or fluctuation induced displacements of the vortices from their positions in the perfect FLL increase the width of  $n(B)$ . The effect is nearly equivalent to smearing  $n(B)$  by convolution with a Gaussian distribution of fields [47]

$$n(B) = \int \frac{1}{\sqrt{2\pi}\sigma_d} \exp\left[-\frac{1}{2}\left(\frac{B-B'}{\sigma_d}\right)^2\right] n(B') dB', \quad (15)$$

where  $\sigma_d$  is related to the root mean square displacement  $\langle u_l^2 \rangle^{1/2}$  of a vortex line about its average position. From  $\mu$ SR studies on numerous superconductors with 3D-like vortices it has been determined that  $\sigma_d \propto B/\lambda_{ab}^2$ . This simply means that stronger overlap of neighbouring vortices reduces the degree of disorder.

The above treatment is a reasonable approximation of the weak FLL disorder in the 3D ‘Bragg-glass’ phase of a type-II superconductor, in which quasi-long-range translational order and perfect topological order are preserved [70]. Note that a more accurate expression for the variance of the FLL field distribution in the Bragg-glass phase has been derived [71], but has yet to be used for the analysis of  $\mu$ SR measurements. More recently, it has been shown that when disorder is strong enough to produce a 3D ‘vortex-glass’ phase, in which the topological order of the FLL is not retained, the  $\mu$ SR line shape is slightly skewed in the opposite way with a ‘tail’ on the low-field side [72, 73]. In this situation, the disorder cannot be handled in a trivial way.

#### *2D pancake vortices.*

The vortex lines in layered superconductors are generally considered to be comprised of coupled 2D ‘pancake’ vortices. When the interlayer coupling is weak, the vortex lines are very *soft*, and pinning and/or thermal fluctuations of the pancake vortices shorten the high-field tail of  $n(B)$  [14, 74, 75].

There has been some debate on how disorder of the FLL should be treated in  $\mu$ SR studies of high- $T_c$  superconductors. An early  $\mu$ SR study by Harshman *et al.* [76] arrived at the conclusion that point distortions of the vortex lines was significant in highly anisotropic  $\text{Bi}_2\text{Sr}_2\text{CaCu}_2\text{O}_{8+\delta}$ , as evidenced by narrow symmetric  $\mu$ SR line shapes at low temperatures and high magnetic fields. On the other hand, under similar conditions broad asymmetric  $\mu$ SR line shapes were observed for  $\text{YBa}_2\text{Cu}_3\text{O}_y$ , consistent with vortex lines that do not wander significantly along their length. The dimensionality of the vortex lines is dependent on the ratio  $\gamma s/\lambda_{ab}$ , where  $\gamma$  is the mass anisotropy and  $s$  is the spacing between  $\text{CuO}_2$  planes. The observations reported in Ref. [76] are consistent with the fact that  $\gamma$  is nearly two orders of magnitude smaller in optimally doped  $\text{YBa}_2\text{Cu}_3\text{O}_y$  than in  $\text{Bi}_2\text{Sr}_2\text{CaCu}_2\text{O}_{8+\delta}$ . Thus in high- $T_c$  cuprates the picture of weakly coupled 2D pancake vortices should be viewed as a limiting case.

Recently, Harshman *et al.* [77] have asserted that point distortions of the vortex lines in *ultra-clean* samples of  $\text{YBa}_2\text{Cu}_3\text{O}_y$  are as important as in  $\text{Bi}_2\text{Sr}_2\text{CaCu}_2\text{O}_{8+\delta}$ . By fitting the total second moment of the  $\mu$ SR line shape for fully doped  $\text{YBa}_2\text{Cu}_3\text{O}_7$  to a phenomenological model containing two independent parameters for pinning-induced distortions of the FLL, Harshman *et al.*

FIG. 5: Fourier transforms of the TF- $\mu$ SR signal from single crystal  $V_3Si$  at  $T=3.8$  K for applied magnetic fields of  $H=30$  kOe and  $H=50$  kOe directed parallel to the  $[001]$  axis (from data in Ref. [64]). The solid red curve in each panel is a Fourier transform of the fit in the time domain (Note: because of apodization, this is slightly different than the fitted  $n(B)$ , an example of which was shown in figure 2). Also shown are contour plots of the field profile  $B(\mathbf{r})$  obtained from the fits to a GL model. The results are in good agreement with STS measurements on  $V_3Si$  [69].

argued that  $\lambda_{ab}(T, H)$  is consistent with  $s$ -wave superconductivity. However, there are several problems with the analysis of the  $\mu$ SR data in Ref. [77]. Most notably, the second moment of  $n(B)$  is assumed to be given by equation (6), which does not account for the finite size of the vortex cores. Also, both the determined value  $\kappa = \lambda_{ab}/\xi_{ab} = 43.8 \pm 1.8$  and the lowest field ( $B=0.05$  T) considered in Ref. [77] are too small for equation (6) to apply. The smaller value of the second moment found at  $B=0.05$  T in Fig. 2 of Ref. [77] is in fact expected, because at this field  $\langle(\Delta B)^2\rangle$  is more appropriately described by equation (12) of Ref. [27]

$$\langle(\Delta B)^2\rangle = \frac{b\kappa^2 \Phi_0^2}{8\pi^2 \lambda^4}. \quad (16)$$

Although the vortex lines in  $YBa_2Cu_3O_y$  and  $La_{2-x}Sr_xCuO_4$  are certainly more rigid than in  $Bi_2Sr_2CaCu_2O_{8+\delta}$ , they do soften in underdoped samples due to an increase in anisotropy  $\gamma$ . Experiments on oxygen-deficient  $YBa_2Cu_3O_y$  thin films [78, 79] indicate that for applied magnetic fields currently attainable in a TF- $\mu$ SR experiment ( $H=80$  kOe), the FLL remains 3D at low  $T$ , except perhaps in lightly doped samples. However, the dimensionality of the vortex system depends on the degree of sample disorder, which can cause pinning-induced misalignment of the pancake vortices that make up a vortex line. Since  $YBa_2Cu_3O_y$  thin films can be strongly disordered, these experiments are sample dependent and don't necessarily tell the story in clean samples. In fact, recent mutual inductance measurements on severely underdoped thin films indicate that  $YBa_2Cu_3O_y$  is really quasi-2D only near  $T_c$  [30].

The weak field dependence of the Josephson plasma resonance in  $YBa_2Cu_3O_{6.50}$  single crystals at low  $T$  is further evidence that the vortices maintain a 3D character in clean underdoped samples [80]. As for underdoped  $La_{2-x}Sr_xCuO_4$ , it has been argued from a combined  $\mu$ SR and small-angle neutron scattering study of  $La_{1.9}Sr_{0.1}CuO_4$  [72] that the vortex lines remain fairly rigid at low  $T$ .

## VORTEX CORE SIZE

Superconductivity is strongly suppressed in the vortex core. A loose definition of the vortex core size is that it is a region of radius  $r \sim \xi$ , where  $\xi$  is the characteristic length scale for spatial variations of the superconducting order parameter  $\psi$ —*i.e.* the GL coherence length. However, this definition is not particularly satisfactory, especially since GL breaks down at low temperatures. Two alternative definitions of the vortex core size have emerged from numerical solutions of the Bogoliubov-de Gennes and quasiclassical Eilenberger equations. The first comes from the initial slope of the pair potential  $\Delta(r)$  near the centre of the vortex core. Assuming  $\Delta(r) \propto r$  close to the core centre, the core radius may be defined as

$$\xi_1 = \Delta_0 / \lim_{r \rightarrow 0} \frac{\Delta(r)}{r}, \quad (17)$$

where  $\Delta_0 \sim 1/\xi_0$  is the bulk superconducting energy gap at zero temperature, and  $\xi_0$  is the BCS coherence length. As shown in figure 6a,  $r = \xi_1$  is the radius at which the linear slope extrapolates to  $\Delta(r) = \Delta_0$ . The absolute value of the spatial supercurrent density profile  $|j(r)|$  provides



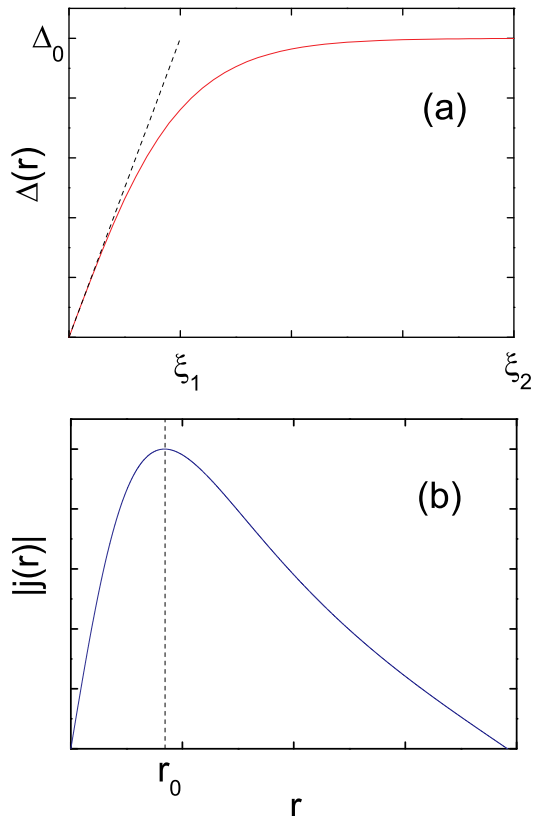


FIG. 6: Spatial variation of (a) the pair potential  $\Delta(r)$  and (b) the absolute value of the supercurrent density  $j(r)$  for an isolated vortex, where  $r$  is the radial distance from the vortex centre.

a second way of defining the core size. As shown in figure 6b,  $|j(r)|$  exhibits a maximum at a distance  $r = r_0$  from the core centre.

### Magnetic field dependence

Figure 7 shows the magnetic field dependence of the vortex core size determined by  $\mu$ SR in the  $\kappa \gg 1$  superconductors  $V_3Si$ ,  $NbSe_2$  and  $LuNi_2B_2C$ . Similar results have been reported for  $CeRu_2$  [53],  $YNi_2B_2C$  [54] and  $Nb_3Sn$  [65]. In agreement with calculations from the quasiclassical Eilenberger equations [81, 82],  $r_0$  and  $\xi_{ab}$  exhibit qualitatively similar dependences on magnetic field. As explained in Ref. [40], the magnetic field dependence of  $r_0$  is partially due to the ‘vortex squeezing effect’—which refers to the increasing overlap of the  $j(r)$  profiles of individual vortex lines with increasing  $H$  (see figure 2 of Ref. [40]).

It is important to stress that the field dependence of the parameter  $\xi_{ab}$  that comes from fits of  $\mu$ SR measurements using the models described in section 4.1, does not mean that the superconducting coherence length is

changing with field. Rather, it simply means that the cutoff factor in these models significantly varies due to changes in the slope of  $\Delta(r)$  in the vortex core region. For this reason the behaviour of  $\xi_{ab}$  is expected to follow that of  $\xi_1$  of equation (17), and hence is considered a measure of the *vortex core size*. In general, the maximum value of the cutoff parameter  $\xi_{ab}$  measured by  $\mu$ SR corresponds to the GL coherence length calculated from  $H_{c2}$  (i.e.  $\xi_{GL} = (\Phi_0/2\pi H_{c2})^{1/2}$ ). At low fields, where the vortices are weakly interacting, the fitted value of  $\xi_{ab}$  more or less agrees with that expected from  $H_{c2}$  (see figure 7).

The observed shrinkage of the vortex cores at higher magnetic fields qualitatively agrees with theoretical calculations for high- $\kappa$  superconductors done in the framework of the quasiclassical Usadel [3, 4] and Eilenberger equations [81, 82]. These theoretical works show that changes in the spatial variation of  $j(r)$  (and hence  $B(r)$ ) and  $\Delta(r)$  with increasing magnetic field are directly related to changes in the electronic structure of the vortex cores that occur with increased vortex-vortex interactions. Physically, the situation is analogous to the electronic band structure that forms when atomic orbitals are combined in a crystal lattice. When atoms come together to form a lattice, the wave functions of the electrons anchored to individual atoms overlap the wave functions of the electrons of neighbouring atoms. This results in the formation of energy bands, which in the case of a metal, leads to delocalized electrons that are capable of carrying electric and thermal currents. In a similar way, as vortices are brought closer together by increasing the applied magnetic field, there is an increased overlap of the wave functions of the single-particle excitations (quasiparticles) bound to an individual vortex [83] with the quasiparticle states of neighbouring vortices [81, 82, 84, 85], resulting in the intervortex transfer of quasiparticles. Since the higher-energy bound quasiparticle core states are more spatially extended, they delocalize first. The reduction of the vortex core size with increasing magnetic field is thus understood as being due to the sequential delocalization of quasiparticle core states, starting with the highest-energy bound state, and terminating with the complete delocalization of the lowest-energy bound state.

While this picture is strongly supported by a comparison of  $\mu$ SR measurements of the vortex core size with the data from other techniques that probe electronic excitations, Kogan and Zhelezina [87] have proposed an alternative theoretical explanation for the field dependence of the core size that is based on weak-coupling BCS theory. Their model predicts that in clean high- $\kappa$  superconductors, the intrinsic superconducting coherence length is not independent of magnetic field, but actually decreases with increasing field. Recently, DeBeer-Schmitt *et al.* [88] measured an unusual field-independent FLL form factor in  $CeCoIn_5$  by small-angle neutron scattering, suggestive of a field-dependent coherence length (see

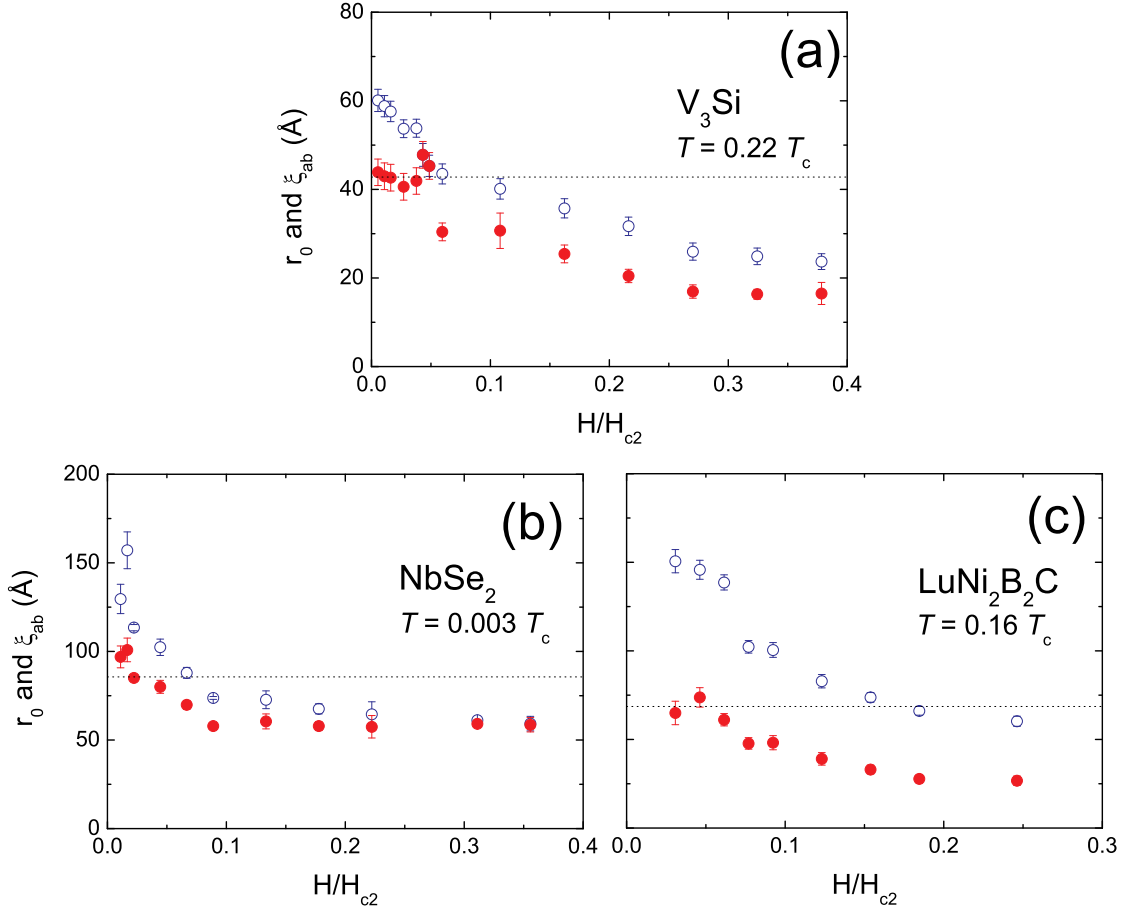


FIG. 7: Magnetic field dependence of  $r_0$  (open circles) and  $\xi_{ab}$  (solid circles) in equation (14) from  $\mu$ SR measurements on single crystals of (a)  $V_3Si$  [64], (b)  $NbSe_2$  [41], and (c)  $LuNi_2B_2C$  [55]. All measurements were done with the applied field parallel to the  $\hat{c}$ -axis. The dotted horizontal line in each panel indicates the value of the GL coherence length  $\xi_{GL}$  calculated from  $H_{c2}(T)$ .

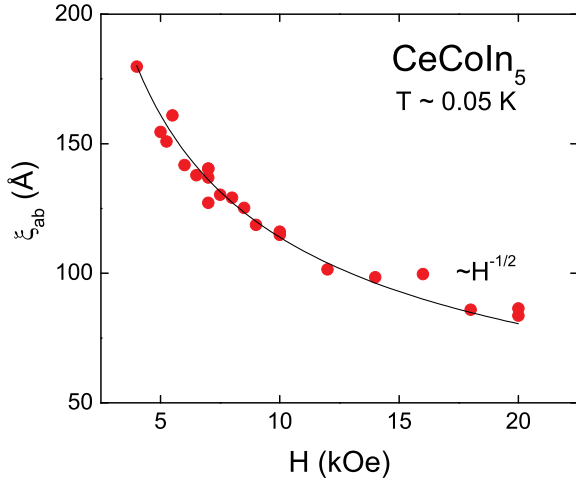


FIG. 8: Magnetic field dependence of the Ginzburg-Landau coherence length inferred from the observation of a field-independent FLL form factor in small-angle neutron scattering measurements on  $CeCoIn_5$  [88].

figure 8). Even so, there may be another explanation for their data that warrants further experimental investigation of the FLL form factor in other materials. A seemingly direct test of the Kogan-Zhelezina theory would be to study the magnetic field dependence of the core size in impurity-doped superconductors. Unfortunately, the addition of impurities is likely to interfere with the inter-vortex transfer of quasiparticles and add disorder to the FLL. Thus the interpretation of such experiments would probably be ambiguous.

### Specific heat

Specific heat measurements are sensitive to both localized and delocalized quasiparticle excitations. In the vortex state the specific heat is usually described by

$$c(T, B) = \gamma(T, B)T + \alpha T^2 + \beta T^3, \quad (18)$$

where the last term  $\beta T^3$  is the phonon contribution. The first term is the electronic contribution to the zero-energy

quasiparticle density of states (DOS)  $N(E=0)$ , *i.e.* the spatial average of the local DOS  $N(E=0, \mathbf{r})$  at the Fermi level  $E=0$ . The ‘Sommerfeld coefficient’ is given as

$$\gamma(B) \equiv \lim_{T \rightarrow 0} c(T, B)/T \propto N(0). \quad (19)$$

The second term in equation (18) is not always clearly present in experimental data, and only recently has theoretical progress in understanding its origin been made. Nakai *et al* [89] have shown there are two electronic contributions to the  $\alpha T^2$  term. The first comes from low-energy states ( $E > 0$ ) that appear near the Fermi energy at  $B \neq 0$ . The second contribution comes from the ‘Kramer-Pesch effect’, which is a shrinking of the vortex cores with decreasing temperature that is associated with the thermal depopulation of the bound quasiparticle core states. As discussed elsewhere [1, 40], the Kramer-Pesch effect has been measured by  $\mu$ SR in a variety of superconductors.

In an isotropic-gapped superconductor, the low-lying excitations are generally considered to be confined to the vortex cores [83]. In this case  $\gamma(B)$  is proportional to the product of the area of a vortex core  $\pi\xi^2$  and the density of vortices [90], so that

$$\gamma(B) \propto \pi\xi^2 B. \quad (20)$$

Thus, if the size of the vortex cores is independent of magnetic field, then  $\gamma(B) \propto B$ . In highly anisotropic-gapped superconductors, including those with line or point nodes at the Fermi surface, the low-lying excitations near the gap minima become the dominate contribution to  $\gamma(B)$ . Volovik showed that for the case of a  $d$ -wave superconductor, the superfluid flow around a vortex lowers the energy of quasiparticles delocalized near the gap nodes, leading to a finite DOS at the Fermi energy and a corresponding nonlinear field dependence for  $\gamma(B)$  [91]. For the case of a highly anisotropic energy gap without nodes, such behavior is expected only if the energy shift exceeds the gap minimum. Until recently, this is more or less how specific heat measurements on type-II superconductors as a function of magnetic field were interpreted.  $\gamma(B) \propto B$  behaviour was indicative of conventional  $s$ -wave superconductivity, and a sublinear dependence of  $\gamma(B)$  on field, usually  $\gamma \propto \sqrt{B}$ , meant unconventional superconductivity.

In 1999 it became clear that the delocalization of quasiparticles brought about by vortex-vortex interactions shows up in the field dependence of the specific heat of  $s$ -wave superconductors—often mimicking the behaviour expected for an unconventional pairing-state symmetry. Theoretically it was shown from solutions of the quasiclassical Eilenberger equations at  $T = 0.5T_c$  that the zero-energy DOS per vortex  $N(0)/B$  depends on magnetic field [81]. In the same work this unexpected behaviour was shown to be due to a shrinking of the vortex cores with increasing field, associated with an increased

overlap of the zero-energy DOS of one vortex with that of its neighbours. This idea was experimentally verified in the same year by relating the field dependence of the vortex core size measured in NbSe<sub>2</sub> by  $\mu$ SR [3] to the field dependence of the specific heat of this material [92].

More recent calculations in the framework of the quasiclassical Eilenberger theory [93] show that for an  $s$ -wave superconductor at  $T = 0.1T_c$ , the isolated vortex behaviour  $\gamma(B) \propto B$  is in fact realized at low temperatures up to a crossover field  $B^*$ . Above  $B^*$ ,  $\gamma(B)$  has a sublinear dependence on field due to the overlap of the low-energy quasiparticle core states from neighbouring vortices. Even so, it is rare to find superconducting materials that exhibit  $\gamma(B) \propto B$  behaviour at low magnetic fields, because any anisotropy of the superconducting energy gap or Fermi surface reduces the value of  $B^*$ . This also means that the vortex core size measured by  $\mu$ SR will most often be dependent on field. Recently, this was shown to be the case even at low field in the marginal type-II superconductor V [42]. The field dependence of the core size in pure V cannot be explained by the theory of Ref. [87], which does not apply to low- $\kappa$  superconductors. On the other hand, an explanation in terms of delocalized core states is compatible with the sublinear dependence of  $\gamma(B)$  on  $B$  found immediately above  $H_{c1}$  in the low- $\kappa$  type-II superconductor Nb [94].

### Thermal conductivity

In contrast to the electronic contribution to the specific heat in the mixed state, the electronic contribution to heat transport comes entirely from extended or delocalized quasiparticles. In superconductors with extreme gap anisotropy, such as LuNi<sub>2</sub>B<sub>2</sub>C [95] or YBa<sub>2</sub>Cu<sub>3</sub>O<sub>y</sub> [96], the dominant contribution to the field dependence of the thermal conductivity at low  $T$  is the Doppler shift of the quasiparticle spectrum outside the vortex cores due to the circulating supercurrents [97, 98]. However, for an  $s$ -wave superconductor, the field dependence of the electronic thermal conductivity  $\kappa_e$  obtained by extrapolating measurements to  $T \rightarrow 0$  K is a direct measure of the delocalization of quasiparticle states bound to the vortex cores.

In recent years,  $\mu$ SR measurements on  $s$ -wave superconductors have established a direct correlation between the field dependence of the vortex core size and the delocalization of quasiparticle core states as measured by thermal conductivity. By imposing the following simple model, excellent agreement between these two very different kinds of measurements has been demonstrated [41]:

The electronic thermal conductivity  $\kappa_e$  is proportional to the zero-energy density of *delocalized* states  $N_{\text{deloc}}(0)$ , and hence grows as the zero-energy density of bound

cores states  $N(0)$  decreases. Since  $N(0)$  is proportional to  $\pi\xi^2 B$ , then

$$\kappa_e \propto N_{\text{deloc}} \propto (\pi\xi(B_{c1})^2 - \pi\xi(B)^2)B, \quad (21)$$

where  $\pi\xi(B_{c1})^2$  and  $\pi\xi(B)^2$  are the areas of the vortex core at  $B=B_{c1}$  and  $B>B_{c1}$ , respectively.

*V<sub>3</sub>Si: a good standard.*

In 2004, a  $\mu$ SR study of  $n(B)$  in the mixed state of the high- $\kappa$   $s$ -wave superconductor V<sub>3</sub>Si was reported [64]. The results of this experiment provide a good standard for comparison of  $\mu$ SR measurements on more complicated systems. The reason is that at low field, the electronic states remain fairly well localized within the vortex cores. Consequently,  $\kappa_e(T \rightarrow 0, H)$  increases slowly with increasing magnetic field [99],  $c(T \rightarrow 0, H)$  is dominated by localized electronic states at low  $H$ , and the vortex core size determined by  $\mu$ SR is essentially independent of  $H$  up to  $H \approx 7.5$  kOe. As shown in figure 9a, equation (21) accurately describes the thermal conductivity data using the  $\mu$ SR values of the vortex core size  $\xi_{ab}$ .

*V and Nb: marginal type-II superconductors.*

As mentioned earlier, the vortex core size in the low- $\kappa$  superconductor V was recently measured by  $\mu$ SR [42]. With the magnetic field applied parallel to the  $\langle 111 \rangle$  direction of a V single crystal, the vortex core size was found to decrease immediately above the lower critical field  $H_{c1} \approx 1$  kOe. The high degree of delocalization of quasiparticle core states necessary to cause the observed shrinking of the vortex core size at such low field is a consequence of the large superconducting coherence length ( $\sim 300$  Å) and 10 % to 20 % gap anisotropy.

While there are no reported measurements of  $\kappa_e(T \rightarrow 0, H)$  for V, there are for the related elemental superconductor Nb [100]. The electronic thermal conductivity of Nb reported in Ref. [100] behaves much like that of V<sub>3</sub>Si, exhibiting a weak exponential increase above  $H_{c1}$ . This is clearly at odds with the  $\mu$ SR results for V. However, it is also at odds with the specific heat measurements of Nb reported in Ref. [94], which indicate an appreciable overlap of the quasiparticle core states of neighbouring vortices immediately above  $H_{c1}$ . As argued in Ref. [94], this discrepancy is due to the way in which these experiments were done. When the electronic specific heat of Nb was measured under zero-field cooled conditions, no appreciable contribution from localized or delocalized quasiparticle states was observed at fields near  $H_{c1}$ . This is consistent with the thermal conductivity data of Ref. [100] measured in monotonically increasing and decreasing magnetic field. On the other hand, under the same field-cooled conditions implemented in the

$\mu$ SR study of V, the specific heat measurements are consistent with delocalized quasiparticle states immediately above  $H_{c1}$ . These experiments show that the intervortex transfer of quasiparticles is disrupted when the FLL is highly disordered. While a well-ordered FLL forms in the sample under field-cooled conditions, flux entry into the sample is impeded by the Bean-Livingston barrier under zero-field cooled or monotonically increasing field conditions. The field dependence of  $\kappa_e(T \rightarrow 0, H)$  has yet to be measured in Nb or V under field-cooled conditions.

*NbSe<sub>2</sub>: multi-band superconductivity.*

For a long time the mixed state of NbSe<sub>2</sub> was considered an archetype of the FLL in conventional type-II superconductors. However, over the past 6 years a number of experiments on NbSe<sub>2</sub> have provided strong evidence for distinct energy gaps on different Fermi sheets [99, 101, 102]. While there is some debate over whether the smaller energy gap resides on the Se or Nb Fermi sheets [103], the experimental signatures of multi-band superconductivity are similar to those of MgB<sub>2</sub>.

Extending theoretical work on MgB<sub>2</sub> [104, 105, 106, 107] to the case of NbSe<sub>2</sub>, suggests that the nonlinearity of  $\gamma(B)$  observed at low  $B$  can be attributed to the occurrence of a smaller energy gap  $\Delta_0$  on one of the Fermi surfaces. In these theories the electronic states of a vortex are dependent on the combined contributions from two different bands, characterized by large and small superconducting energy gaps and different Fermi surface anisotropies. At low magnetic field the dominant contribution to the low-energy quasiparticle core states comes from the small-gap band. Because of the small size of the energy gap, these core states are loosely bound to the vortex and easily delocalize via overlap with the low-energy core states of neighbouring vortices. Consequently, the vortex core is large at low field, and shrinks with increasing magnetic field. However, in contrast to a single-band superconductor, low-energy quasiparticle states continue to be localized around the the vortex cores at high fields due to the contribution from the large-gap band. In particular, the large-gap band results in electronic states that are more confined to the vortex core. While the electronic vortex core states of the individual bands can be probed separately by STS [108], this does not imply that there are two different kinds of vortices separated in real space. Both bands contribute to a single vortex, but the magnetic field dependence of each contribution is different. Moreover, the energy gaps of the two bands are related in the sense that only a single superconducting transition occurs.

In a  $\mu$ SR study of NbSe<sub>2</sub> at  $T=0.02$  K, in which thermal excitations of the bound quasiparticle core states are largely frozen out, Callaghan *et al.* [41] explicitly detected large vortex cores at low magnetic fields (see fig-

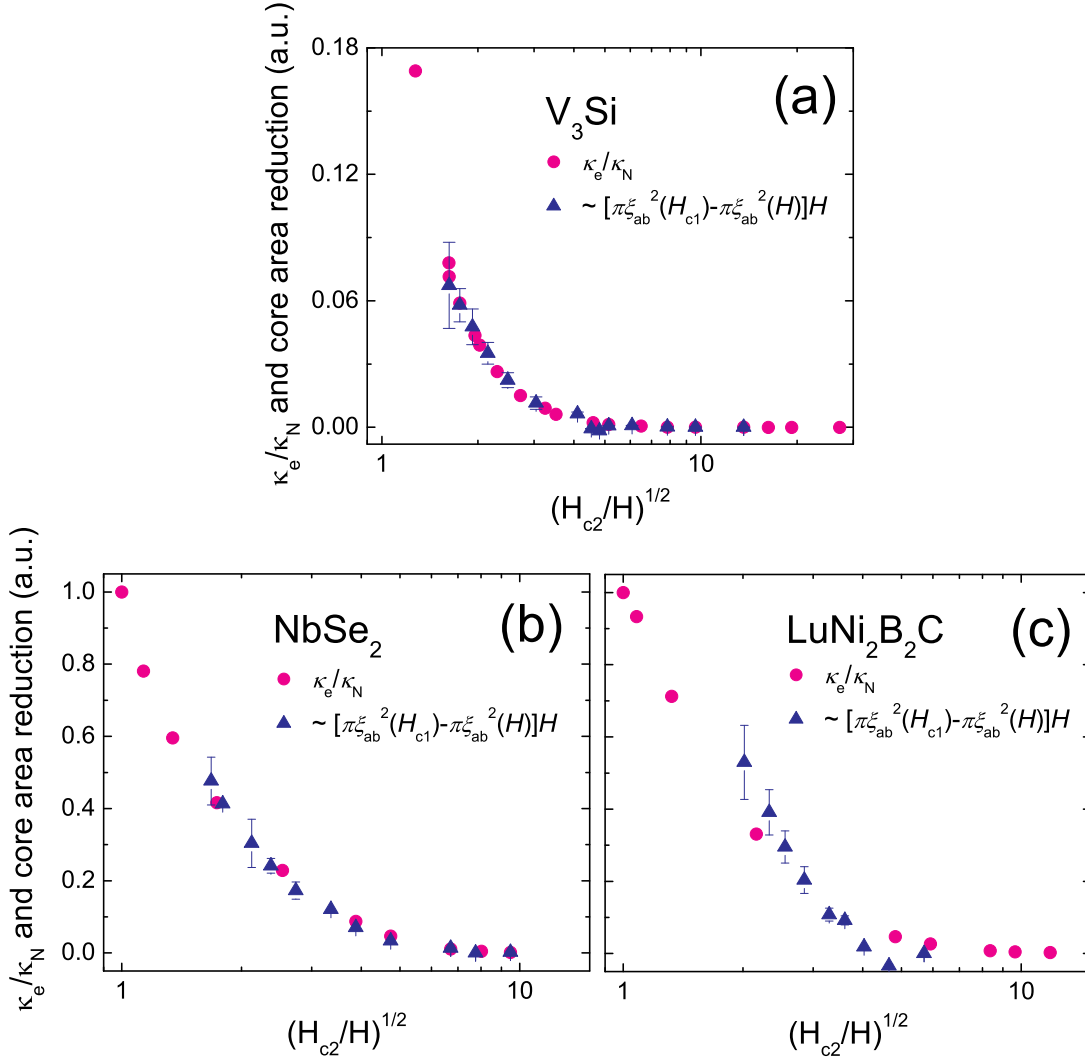


FIG. 9: (a)  $\mu$ SR [64] and electronic thermal conductivity [99] data for  $V_3Si$ . The electronic thermal conductivity data (solid circles) is normalized to the value  $\kappa_N$  at  $H_{c2}$ . The  $\mu$ SR data (solid triangles) is plotted as equation (21). (b) Equivalent  $\mu$ SR [41] and electronic thermal conductivity [99] data for  $NbSe_2$ . (c) Equivalent  $\mu$ SR [55] and electronic thermal conductivity [95] data for  $LuNi_2B_2C$ .

ure 10). With increasing  $H$  the core size rapidly shrinks. This behaviour is attributed to the ease at which the loosely bound core states delocalize via their overlap with the core states of neighbouring vortices. As shown in figure 10, the core size saturates above  $H \approx 0.1H_{c2}$ . At these fields the experiment probes the smaller vortices associated with the large-gap band. The saturation of the core size reflects the reluctance of the tightly bound core states of these smaller vortices to delocalize. This interpretation of the  $\mu$ SR measurements is in accord with what is known about the vortices in  $MgB_2$ . At fields far below  $H_{c2}$ , Eskildsen *et al.* [108] detected vortices in  $MgB_2$  by STS that have a large core size relative to estimates from  $H_{c2}$  and do not have localized core states. This is consistent with the full field dependence of the core size inferred from specific heat measurements [109].

The unavailability of single crystals of sufficient size has so far prevented a study of  $\xi_{ab}(H)$  in  $MgB_2$  by  $\mu$ SR.

The two-gap interpretation of the field dependence of the core size in  $NbSe_2$  is also supported by a remarkable agreement with the field dependence of  $\kappa_e(T \rightarrow 0, H)$  measured independently in Ref. [99] (see figure 9b). In contrast to  $V_3Si$ ,  $\kappa_e(T \rightarrow 0, H)$  rises rapidly with increasing field just above  $H_{c1}$ , indicating the presence of highly delocalized quasiparticle states. This is the same behaviour that is observed for the electronic thermal conductivity of  $MgB_2$  [110] and the heavy-fermion compound  $PrOs_4Sb_{12}$  [111, 112], and is understood to arise from two or more superconducting energy gaps. As is the case for  $MgB_2$ , intermediate size single crystals of  $PrOs_4Sb_{12}$  are not yet available for  $\mu$ SR studies, and hence the field dependence of the vortex core size has not

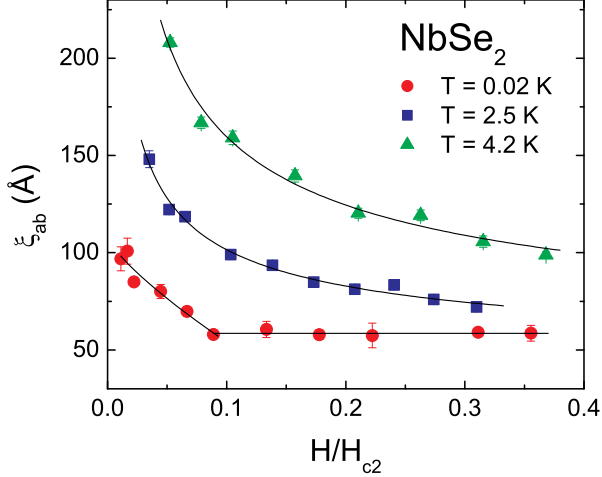


FIG. 10: Magnetic field dependence of the cutoff parameter  $\xi_{ab}$  from  $\mu$ SR measurements on single crystals of  $\text{NbSe}_2$  at different temperatures [3, 41].

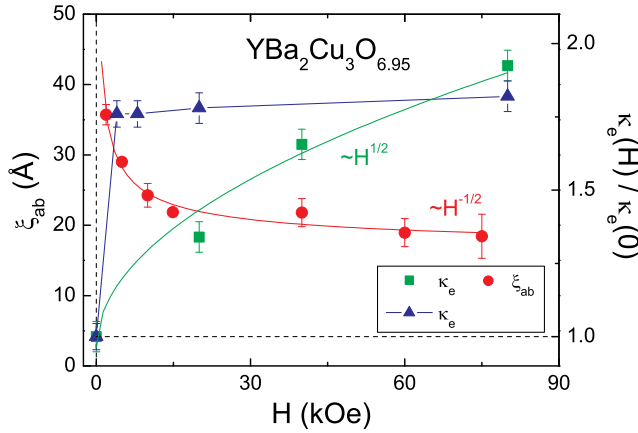


FIG. 11: The magnetic field dependence of  $\xi_{ab}$  in  $\text{YBa}_2\text{Cu}_3\text{O}_{6.95}$  determined by  $\mu$ SR [38] and the normalized electronic thermal conductivity  $\kappa_e(H)/\kappa_e(0)$  measured in  $\text{YBa}_2\text{Cu}_3\text{O}_{6.9}$  by Chiao *et al.* [96] and in  $\text{YBa}_2\text{Cu}_3\text{O}_7$  by Hill *et al.* [115], respectively. All data are extrapolations to  $T \rightarrow 0$  K. Note, the field dependence of  $\xi_{ab}$  shown here is a more accurate analysis of the measurements of Ref. [38]. In particular, the modified Bessel function  $K_1(u)$  in equation (14) was calculated numerically, whereas the analysis of Ref. [38] assumed the following analytical approximation:  $K_1(u) = (\pi/2u)^{1/2} \exp(-u)$ , valid for  $u \gg 1$ .

been measured.

#### *YBa<sub>2</sub>Cu<sub>3</sub>O<sub>y</sub>: highly anisotropic and multiple gaps?*

As shown in figure 11, the vortex-core size in the high- $T_c$  superconductor  $\text{YBa}_2\text{Cu}_3\text{O}_{6.95}$  [38] shrinks with

increasing magnetic field, such that  $\xi_{ab}(H) - \xi_{ab}(0) \propto H^{-1/2}$ . At first glance this behaviour resembles the previous examples, where the shrinking of the vortex cores has been associated with the delocalization of quasiparticle core states. However, in  $\text{YBa}_2\text{Cu}_3\text{O}_y$  the low-energy quasiparticle core states are expected to be extended along the nodal directions of the  $d_{x^2-y^2}$ -wave gap function [59, 82], and hence are already delocalized at low field. Furthermore, the value of  $\xi_{ab}$  deduced by  $\mu$ SR at low  $H$  seems rather large. As discussed in Ref. [40], the large vortex-core size at low  $H$  appears to be unique among the cuprates and likely results from *proximity-induced* superconductivity on the  $\text{CuO}$  chains. Calculations by Atkinson [113] show that large two-fold symmetric vortices result from coupling of the  $\text{CuO}$  chain and  $\text{CuO}_2$  plane layers (see figure 12). The vortex core size in  $\text{YBa}_2\text{Cu}_3\text{O}_{6.95}$  saturates near  $H = 40$  kOe, at which the FLL begins a gradual hexagonal-to-square transition [114]. The  $d_{x^2-y^2}$ -wave superconducting order parameter is predicted to produce fourfold symmetry in the spatial field profile  $B(\mathbf{r})$  around the vortex cores [59]. Thus the fourfold symmetry of the FLL at high fields likely results from strong overlap of the intrinsic  $d_{x^2-y^2}$ -wave vortices.

A comparison of the  $\mu$ SR data to electronic thermal conductivity measurements by Chiao *et al.* [96] seems to imply that there are bound core states which delocalize with increasing magnetic field (see figure 11). However, the behaviour of  $\kappa_e(H)$  is more likely due to a field-induced Doppler shift of the quasiparticle spectrum outside the vortex cores [97, 98]. More recent measurements on ultraclean single crystals of  $\text{YBa}_2\text{Cu}_3\text{O}_7$  by Hill *et al.* [115] show a saturation of  $\kappa_e(H)$  at low  $H$ , argued to indicate an exact cancellation of the contributions from the Doppler shift and scattering of the quasiparticles by the vortices. Thus, consistent with a highly anisotropic gap, there is no established correlation between the size of the vortex cores and electronic thermal conductivity measurements on very clean samples.

#### *RNi<sub>2</sub>B<sub>2</sub>C: highly anisotropic or multiple gaps?*

For some time now, experimental evidence has mounted that the superconducting energy gap in rare-earth nickel borocarbides  $\text{RNi}_2\text{B}_2\text{C}$  ( $R \equiv \text{Dy, Ho, Er, Tm, Lu}$  and  $\text{Y}$ ) is highly anisotropic, with line or point nodes. For example, thermal conductivity measurements on  $\text{LuNi}_2\text{B}_2\text{C}$  reveal the existence of highly delocalized quasiparticles above  $H_{c1}$  [95]. However, there is also evidence suggesting that these borocarbide materials exhibit multi-band superconductivity [116, 117, 118, 119]. Figure 9c shows that unlike  $\text{YBa}_2\text{Cu}_3\text{O}_y$ , for  $\text{LuNi}_2\text{B}_2\text{C}$  there is good agreement between  $\mu$ SR measurements of the vortex core size and the field dependence of the electronic thermal conductivity. This indicates that there are quasiparticle vortex-core states at low temperatures

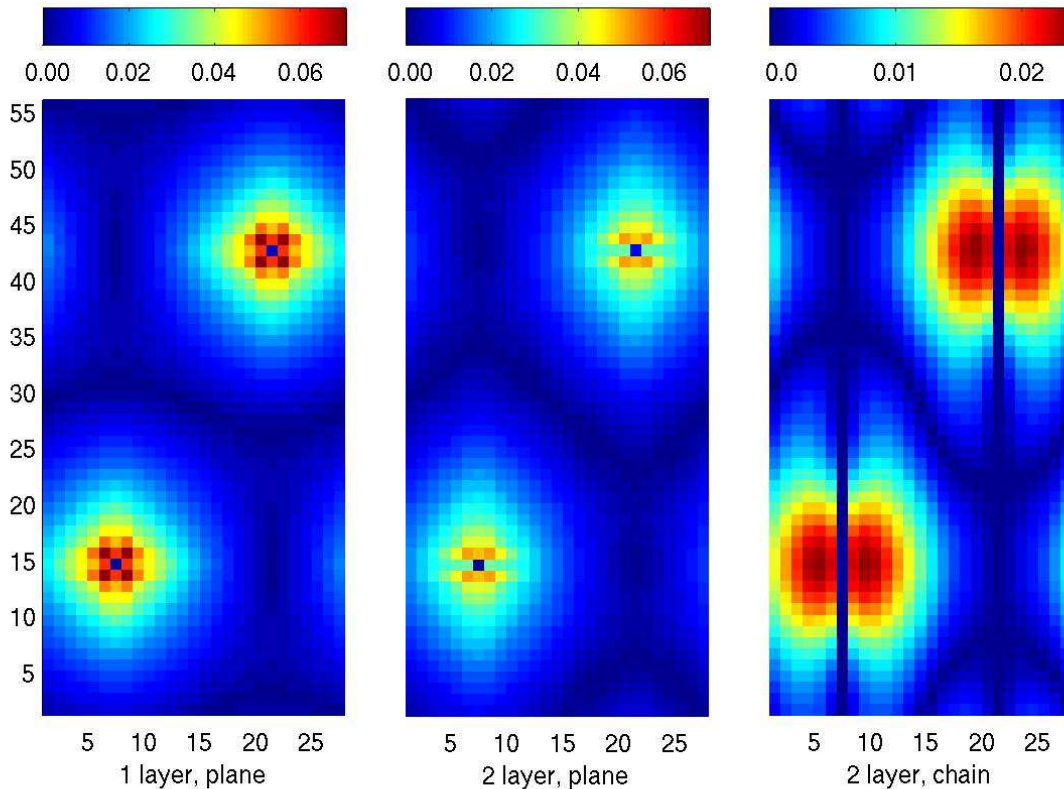


FIG. 12: Contour plot of the spatial dependence of the magnitude of the supercurrent density  $j(\mathbf{r})$  for vortices in a single-layer  $d_{x^2-y^2}$ -wave superconductor (left) calculated from self-consistent solutions of the Bogoliubov de Gennes equations [113]. Also shown are the results of similar calculations for a 2 layer superconductor, consisting of a *chain* layer coupled to a single  $d_{x^2-y^2}$ -wave superconducting *plane*. The middle panel shows what the vortices look like on the plane layer, and the right panel shows what they look like on the chain layer.

that delocalize with increasing magnetic field. Since the anisotropy of the superconducting energy gap manifests itself in the electronic structure of the vortices, the superconducting gap of  $\text{LuNi}_2\text{B}_2\text{C}$  must be less anisotropic than in  $\text{YBa}_2\text{Cu}_3\text{O}_y$ . Moreover, measurements done to date are not inconsistent with multiple superconducting gaps. The  $\mu\text{SR}$  measurements on  $\text{LuNi}_2\text{B}_2\text{C}$  by Price *et al.* [55] only extend down to  $T = 2.5$  K. As in the case of  $\text{NbSe}_2$ , a clear signature of multiple-gap superconductivity might be seen in the field dependence of the vortex-core size at lower temperatures, where thermal excitations of the quasiparticle core states are largely frozen out. Interestingly,  $\mu\text{SR}$  measurements of  $\xi_{ab}(H)$  in  $\text{YNi}_2\text{B}_3\text{C}$  at  $T = 3$  K by Ohishi *et al.* [54] display a clear saturation above  $H \approx 5$  kOe indicative of a second superconducting gap.

#### Magnetic field dependence of $\lambda_{ab}$

It is important to stress that the field dependence of the fit parameter  $\lambda_{ab}$  generally does not imply that the superfluid density depends on field. Instead it is an indication that the theoretical model for  $n(B)$  does not contain all of the relevant physics. On the other hand, a “true” measure of the *magnetic penetration depth* in a  $\mu\text{SR}$  experiment has been demonstrated to be given by the  $H \rightarrow 0$  extrapolated value of  $\lambda_{ab}$  [41, 42]. In other words, when an inadequate model for  $n(B)$  is used to fit the TF- $\mu\text{SR}$  signal, the difference between  $\lambda_{ab}$  and the magnetic penetration depth grows with increasing magnetic field. This has been nicely demonstrated in several theoretical works [37, 39, 43, 44].

The *effective* length scale  $\lambda_{ab}$  measured by  $\mu\text{SR}$  in the vortex state of single-crystal superconductors usually exhibits a strong dependence on magnetic field at low temperatures. This was first observed in  $\text{YBa}_2\text{Cu}_3\text{O}_{6.95}$  single crystals [52], where it was attributed to effects asso-

ciated with the high anisotropy of the  $d_{x^2-y^2}$ -wave superconducting energy gap  $\Delta(\mathbf{k})$ . There are two primary effects of strong gap and/or Fermi surface anisotropy on  $\lambda_{ab}$ :

- A nonlinear supercurrent response to the applied field  $H$  results from a quasi-classical ‘Doppler’ shift of the quasiparticle energy spectrum by the flow of superfluid around a vortex [91]. When the Doppler shift exceeds the energy gap, Cooper pairs are broken, and  $\lambda$  increases. Nonlinear effects are particularly strong in a  $d_{x^2-y^2}$ -wave superconductor, where even at low  $T$  and weak  $H$  pair breaking occurs from the excitation of quasiparticles at the gap nodes. A sizeable nonlinear response can also occur in  $s$ -wave superconductors that have a highly-anisotropic energy gap, a smaller energy gap on one of the Fermi sheets (*i.e.* a multi-band superconductor), and/or a highly-anisotropic Fermi surface.
- A nonlocal supercurrent response to the applied field  $H$  occurs in the limit  $\lambda \ll \xi_0$ , meaning that the supercurrent density  $\mathbf{j}(\mathbf{r})$  depends on the magnetic vector potential  $\mathbf{A}(\mathbf{r})$  within a volume of radius  $\sim \xi_0$  around  $\mathbf{r}$ . Since  $\xi_0 = \hbar v_F / \pi \Delta$ , the value of the superconducting coherence length is  $\mathbf{k}$ -dependent, *i.e.* it is dependent on both the energy gap  $\Delta(\mathbf{k})$  and the Fermi velocity  $v_F(\mathbf{k})$ . In a  $d_{x^2-y^2}$ -wave superconductor, nonlocal effects arise from the divergence of  $\xi_0(\mathbf{k})$  at the gap nodes, but they may also occur in isotropic-gapped superconductors having strong Fermi surface anisotropy. In either situation, the nonlocal response vanishes far from the vortex cores, so that only the spatial distribution of magnetic field in and around the vortex cores is influenced.

In 1999, a high-field TF- $\mu$ SR study of  $\text{YBa}_2\text{Cu}_3\text{O}_{6.95}$  [38] showed that  $\lambda_{ab}(H)$  has a sublinear dependence on  $H$ , in apparent agreement with theoretical predictions for nonlocal and nonlinear effects in the vortex state of a  $d_{x^2-y^2}$ -wave superconductor [37]. In this case the dominant contribution to the field dependence of  $\lambda_{ab}(H)$  are nonlocal effects. With increasing  $H$ , the increased overlap of the spatial regions around the vortex cores characterized by a nonlocal response, reduces the width of the  $\mu$ SR line shape. Since the phenomenological GL and London models for  $B(\mathbf{r})$  do not account for this, the fitted value of  $\lambda_{ab}$  exceeds the actual magnetic penetration depth.

There have been several  $\mu$ SR studies on systems that exhibit field-induced hexagonal-to-square FLL transformations, where the  $\mu$ SR signals have been fit assuming a phenomenological London model developed by Kogan *et al.* [60, 61]. The Kogan model includes nonlocal corrections that stem from Fermi surface anisotropy. As shown in figure 13, the Kogan model adequately accounts for

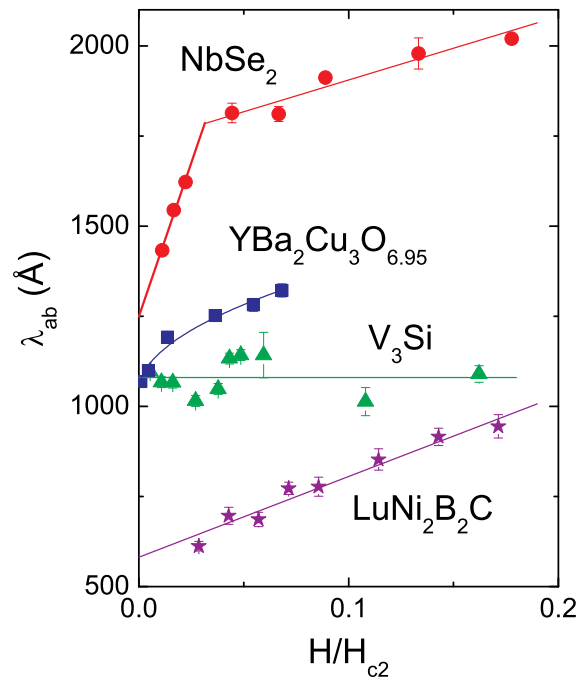


FIG. 13: Magnetic field dependence of the fitting parameter  $\lambda_{ab}$  plotted versus reduced field for  $\text{LuNi}_2\text{B}_2\text{C}$  [55],  $\text{V}_3\text{Si}$  [64],  $\text{NbSe}_2$  [41] and  $\text{YBa}_2\text{Cu}_3\text{O}_{6.95}$  [92]. The reduced field for  $\text{YBa}_2\text{Cu}_3\text{O}_{6.95}$  assumes  $H_{c2} = 1100$  kOe, as determined in Ref. [120]. The results for  $\text{V}_3\text{Si}$  and  $\text{LuNi}_2\text{B}_2\text{C}$  come from fits to the ‘Kogan model’ [60, 61] that includes nonlocal effects, whereas the data for  $\text{NbSe}_2$  and  $\text{YBa}_2\text{Cu}_3\text{O}_{6.95}$  come from fits assuming an analytical GL model [23].

nonlocal effects in  $\text{V}_3\text{Si}$  at low field, as the fitted  $\lambda_{ab}$  is field-independent. The same model has also been applied to  $\mu$ SR measurements on borocarbide superconductors [54, 55] and  $\text{Nb}_3\text{Sn}$  [65]. However, in these cases  $\lambda_{ab}$  still exhibits a field dependence. This suggests that there is a highly anisotropic superconducting gap (or multiple gaps) that causes the field dependence of  $\lambda_{ab}$ —which in turn indicates that the theoretical model fails to accurately portray the field distribution of the FLL.

Kadono [121] has argued that the field dependence of  $\lambda_{ab}$  measured by  $\mu$ SR in any type-II superconductor is indicative of the degree of anisotropy of the superconducting order parameter. This seems to be true, although  $\lambda_{ab}(H)$  is partly influenced by changes in the field decay outside the vortex core arising from an increased overlap of the quasiparticle core states of neighbouring vortices. Some examples of the field dependence of  $\lambda_{ab}$  obtained in  $\mu$ SR studies are shown in figure 13. For the case of  $\text{V}_3\text{Si}$ , where the quasiparticles are tightly bound to the vortex cores at low reduced field  $H/H_{c2}$ ,  $\lambda_{ab}$  is at most weakly dependent on field. The Fermi surface anisotropy responsible for the square FLL that occurs at higher fields does not affect  $\lambda_{ab}(H)$  at low field. On the other hand, the rapid delocalization of quasiparticles in  $\text{NbSe}_2$  with



increasing magnetic field appears to influence  $\lambda_{ab}(H)$ , as it exhibits a stronger field dependence than what is observed in highly anisotropic  $\text{YBa}_2\text{Cu}_3\text{O}_{6.95}$ . Recently, Laiho *et al.* [44] have shown that the field dependences of  $\lambda_{ab}$  in  $\text{V}_3\text{Si}$  and  $\text{NbSe}_2$  vanish if an appropriate temperature and field-dependent cutoff function numerically calculated from the quasiclassical Eilenberger equations for an  $s$ -wave superconductor is used to fit the  $\mu\text{SR}$  measurements. This is because the low-energy excitations of the vortex cores that affect the field distribution are handled by the quasiclassical Eilenberger theory. While the magnetic penetration depth of an isotropic  $s$ -wave superconductor in the vortex state has no appreciable field dependence in the microscopic theory, the vortex core size has a strong field dependence due to the intervortex transfer of quasiparticles [81, 82].

## MAGNETISM IN HIGH- $T_c$ SUPERCONDUCTORS

At the turn of the 21<sup>st</sup> century, neutron scattering, NMR and  $\mu\text{SR}$  experiments on high- $T_c$  superconductors revealed that the application of a magnetic field may induce or enhance antiferromagnetic (AF) spin correlations. In many cases, the AF spin correlations are most pronounced in and around the vortex cores where superconductivity is suppressed. These findings suggest there is a competing magnetic order that coexists with superconductivity. However, the theoretical implications of this hinge on some important details about the experiments, such as whether the observed magnetism is static (or quasistatic) or dynamic, and whether or not static (or quasistatic) magnetism is also present in zero magnetic field.

### Magnetism in zero applied magnetic field

High- $T_c$  superconductivity emerges from the gradual destruction of the insulating AF parent compound by the doping of charge carriers into the  $\text{CuO}_2$  layers. Shortly after their discovery, zero-field (ZF)  $\mu\text{SR}$  experiments on high- $T_c$  superconductors showed that static electronic moments are still present in lightly-doped superconducting samples at low temperatures. In particular, an early ZF- $\mu\text{SR}$  study of  $\text{YBa}_2\text{Cu}_3\text{O}_y$  at  $T=90$  mK showed that static magnetism was still present in samples with oxygen content  $y \leq 6.51$ , but not in a  $y=6.54$  sample [122]. Similarly, an early ZF- $\mu\text{SR}$  study of  $\text{La}_{2-x}\text{Sr}_x\text{CuO}_4$  [123] reported static internal fields at low temperature for  $x \leq 0.15$ . While these experiments suggested that static magnetism and superconductivity coexist, there was considerable worry that the samples studied contained an inhomogeneous concentration of copper magnetic moments due to nonuniform doping of holes [124]. Subsequent ZF- $\mu\text{SR}$  experiments on pure  $\text{La}_{2-x}\text{Sr}_x\text{CuO}_4$  indicated that

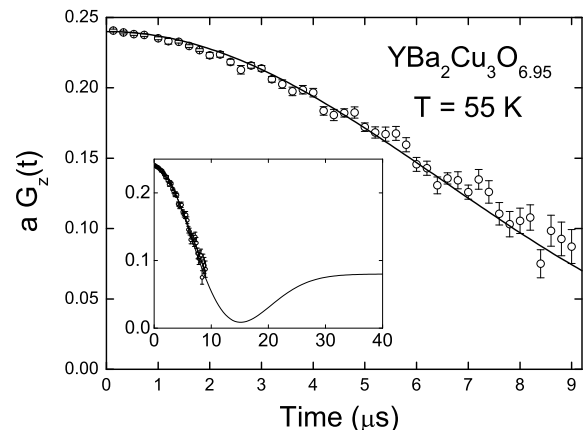


FIG. 14: Time evolution of the muon spin polarization in  $\text{YBa}_2\text{Cu}_3\text{O}_{6.95}$  at  $T=55$  K and  $H=0$ , measured with the initial polarization  $P(0)$  perpendicular to the  $\hat{c}$ -axis [127]. The solid curve is the static Gaussian Kubo-Toyabe function with  $\Delta = 0.1144 \mu\text{s}^{-1}$ . The inset shows what this function looks like beyond the time range of the  $\mu\text{SR}$  signal. Note, the data shown here was obtained using a continuous-wave muon beam at TRIUMF (Vancouver, Canada). With a pulsed muon source, such as that at ISIS (Oxford, United Kingdom), it is very feasible to extend this  $\mu\text{SR}$  spectrum up to 20  $\mu\text{s}$ .

static electronic moments are not present in samples with strontium content as high as  $x=0.15$  [122, 125, 126], although the extrapolated  $T \rightarrow 0$  K critical value of  $x$  for the onset of static magnetism has never been accurately determined. At dopings above where static magnetism is not observed in ZF- $\mu\text{SR}$  experiments, magnetic fluctuations persist that are visible by NMR and inelastic neutron scattering.

Whether the frozen spins observed by ZF- $\mu\text{SR}$  in underdoped superconducting samples coexist with superconductivity or are simply due to phase segregated hole-poor regions, has been a central issue of controversy in the field. Establishing *coexistence* experimentally requires showing that a given sample exhibits both magnetism and superconductivity throughout 100 % of its volume. Since magnetic and non-magnetic regions in the same sample give distinct  $\mu\text{SR}$  signals with amplitudes proportional to the volume of the sample occupied by each phase, in principle  $\mu\text{SR}$  can determine whether magnetism is present in the entire sample. One constraint, however, is imposed by the sensitivity of  $\mu\text{SR}$  to nuclear dipole moments. Randomly orientated nuclear dipoles cause a Gaussian relaxation of the ZF  $\mu\text{SR}$  time signal, as shown in figure 14. The solid curve is a fit to a static Gaussian Kubo-Toyabe function

$$G_z^{\text{KT}}(t) = \frac{1}{3} + \frac{2}{3}(1 - \Delta^2 t^2) \exp(-\frac{1}{2}\Delta^2 t^2), \quad (22)$$

where  $\Delta/\gamma_\mu$  is the width of the Gaussian field distribution at the muon site due to the dense nuclear dipoles

(recall  $\gamma_\mu = 0.0852 \mu\text{s}^{-1}\text{G}^{-1}$ ). Typically,  $\Delta \sim 0.1 \mu\text{s}^{-1}$ , which corresponds to a field of  $\sim 1$  G at the muon site. A muon sitting  $20 \text{ \AA}$  away from a copper atom with a magnetic moment of  $\sim 1 \mu_B$  will sense a  $\sim 1$  G field, whereas a muon sitting further away will not detect a field larger than that from the nuclear dipoles. Thus if all muons implanted in the sample experience a local magnetic field  $> 1$  G, the nonmagnetic hole-rich regions cannot be larger than  $\sim 20 \text{ \AA}$ . This conclusion was reached by Niedermayer *et al.* [125] in ZF- $\mu$ SR studies of the  $\text{La}_{2-x}\text{Sr}_x\text{CuO}_4$  and  $\text{Y}_{1-x}\text{Ca}_x\text{Ba}_2\text{Cu}_3\text{O}_6$  systems, where the hole doping in the  $\text{CuO}_2$  layers is controlled by cation substitution. Kanigel *et al.* [128] also concluded from ZF- $\mu$ SR measurements that phase separation in  $(\text{Ca}_x\text{La}_{1-x})(\text{Ba}_{1.75-x}\text{La}_{0.25+x})\text{Cu}_3\text{O}_y$  is on a microscopic scale. The maximum size of the nonmagnetic hole-rich regions inferred from these experiments is nearly equivalent to the minimum possible spatial extent of the superconducting regions. The latter is set by the superconducting coherence length  $\xi_0$ , which is typically  $15\text{-}20 \text{ \AA}$  in high- $T_c$  superconductors. Thus, the length scale of these ZF- $\mu$ SR experiments is almost, but not quite small enough to determine whether magnetism and superconductivity coexist in the same spatial region.

While the ZF- $\mu$ SR studies of Refs. [125, 128] provided strong evidence for the coexistence of magnetism and superconductivity on a nano-scale level, a couple of questions about these works have lingered. The first is whether superconductivity occurs in the entire bulk of the sample. The second question is whether the inherent cation disorder that is present in the systems studied in Refs. [125, 128] is responsible for the occurrence of electronic moments in superconducting samples. To address these questions, more recently, ZF- $\mu$ SR, TF- $\mu$ SR and bulk magnetization measurements were performed on both high-quality polycrystalline samples [129] and single crystals [130] of  $\text{YBa}_2\text{Cu}_3\text{O}_y$ . In contrast to the systems studied in Refs. [125, 128], hole doping in  $\text{YBa}_2\text{Cu}_3\text{O}_y$  is done by varying the oxygen concentration in the  $\text{CuO}$  chain layers, rather than by cation substitution. While superconductivity is widely believed to take place within the  $\text{CuO}_2$  planes, the chains themselves are conductive and superconducting [131, 132], due to strong coupling with the nearby  $\text{CuO}_2$  planes [133, 134]. Furthermore, charge ordering in the  $\text{CuO}$  chain layers induces charge-density modulations in the  $\text{CuO}_2$  layers [135]. Precision ZF- $\mu$ SR measurements on  $\text{YBa}_2\text{Cu}_3\text{O}_y$  show that the charge ordering affects the relaxation of the  $\mu$ SR signal [136]. However, this could be due to a change in the nuclear dipole field sensed by the muon, rather than the formation of electronic moments. More importantly, the effects of charge ordering on the ZF- $\mu$ SR spectrum weakens with decreasing oxygen content, making it easy to identify the onset of static electronic moments in lightly doped samples.

The more recent ZF- $\mu$ SR of studies of high-quality

$\text{YBa}_2\text{Cu}_3\text{O}_y$  samples [129, 130] are consistent with the earlier experiments, in that static electronic moments occurring in superconducting samples with a hole-doping concentration less than  $p \approx 0.08$  are sensed by all implanted muons. In samples where  $T_c$  is greater than the onset temperature for static electronic moments, TF- $\mu$ SR measurements above the spin freezing temperature  $T_f$  (or  $T_M$  in Ref. [130]) show that a vortex lattice is formed throughout the bulk of the sample. In other words, the entire sample exhibits superconductivity. Below  $T_f$ , the same conclusion cannot be reached, because the magnetism rapidly depolarizes the TF- $\mu$ SR signal. However, bulk magnetization measurements show no reduction in the superconducting response below  $T_f$ . Thus, the experiments of Refs. [129, 130] appear to establish that static magnetism and superconductivity coexist on a microscopic scale. Saying any more than this goes beyond the spatial resolution of the ZF- $\mu$ SR experiments.

The arrangement of the frozen Cu spins in the coexistence phase inferred from the ZF- $\mu$ SR experiments may be compared to that indicated by neutron scattering experiments. The ZF- $\mu$ SR experiments on  $\text{La}_{2-x}\text{Sr}_x\text{CuO}_4$  [125] show that a cluster spin-glass (CSG) phase persists in the superconducting state and is characterized by an onset temperature that decreases continuously across the insulator-superconducting boundary. The CSG phase, which has also been detected by  $^{139}\text{La}$  nuclear quadrupole resonance (NQR) [137, 138, 139], consists of AF spin correlations within domains that are separated by walls of hole-rich material, with the easy axis of the staggered magnetization uncorrelated between clusters. Neutron scattering experiments on  $\text{La}_{2-x}\text{Sr}_x\text{CuO}_4$  show that both static and dynamic incommensurate spin correlations exist across the insulator-superconducting boundary [140]. The source of the low-temperature *static* incommensurate spin correlations that give rise to an elastic neutron scattering peak shifted with respect to the AF position for  $0.2 \leq x \leq 0.12$  samples [141, 142, 143], is likely the same static (or quasistatic) magnetism detected by the low-frequency  $\mu$ SR and NQR measurements. In fact, Wakimoto *et al.* [143] showed that the ordered magnetic moment decreases continuously across the insulator-superconducting boundary. In recent years, spin-spiral models [144] have emerged to explain the magnetic incommensurability of  $\text{La}_{2-x}\text{Sr}_x\text{CuO}_4$ . Lüscher *et al.* [145] have proposed that the CSG phase observed at low  $T$  by ZF- $\mu$ SR results from the freezing of incompatible spin-spiral configurations in neighbouring  $\text{CuO}_2$  layers.

The ZF- $\mu$ SR signals for  $p < 0.08$  superconducting samples of  $\text{YBa}_2\text{Cu}_3\text{O}_y$  at low temperature are characterized by a rapidly damped oscillation at early times [122, 129, 130]. An example of this is shown in figure 16 for  $\text{YBa}_2\text{Cu}_3\text{O}_{6.37}$ . The rapidly damped oscillation is indicative of very short-range magnetic order. Sanna *et al.* [129] have argued that this is consistent with nanoscale

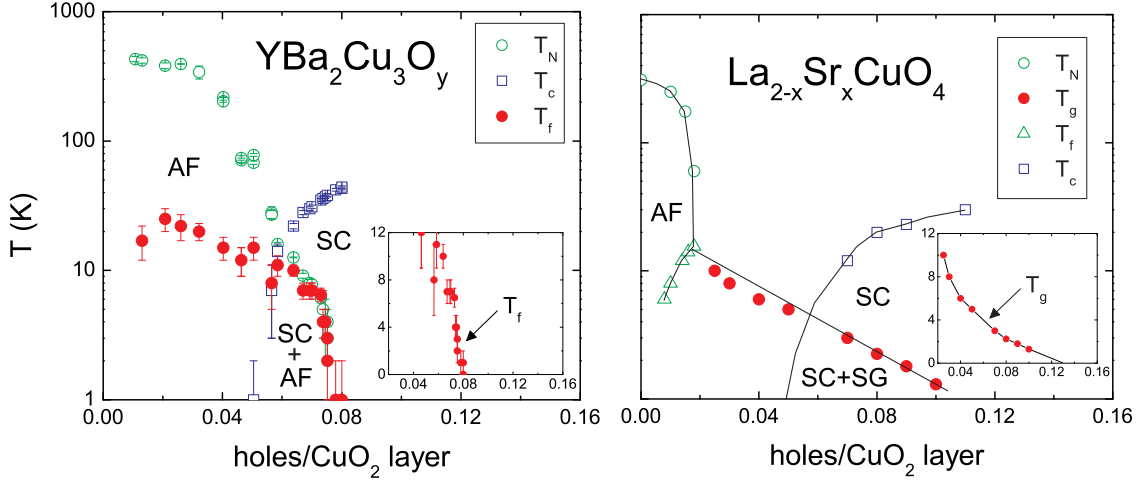


FIG. 15: Magnetic phase diagrams deduced from ZF- $\mu$ SR studies of  $\text{YBa}_2\text{Cu}_3\text{O}_y$  [129] and  $\text{La}_{2-x}\text{Sr}_x\text{CuO}_4$  [125]. In  $\text{YBa}_2\text{Cu}_3\text{O}_y$ , static short-range AF correlations are detected below the spin-freezing temperature  $T_f$ . In  $\text{La}_{2-x}\text{Sr}_x\text{CuO}_4$ , a ‘cluster’ spin-glass (SG) state appears below  $T_g$ . In both materials there is a microscopic coexistence of superconductivity (SC) and frozen AF correlations in underdoped samples. The insets in each panel show the  $T \rightarrow 0$  K extrapolation of the transition temperatures for static magnetism plotted on a linear scale.

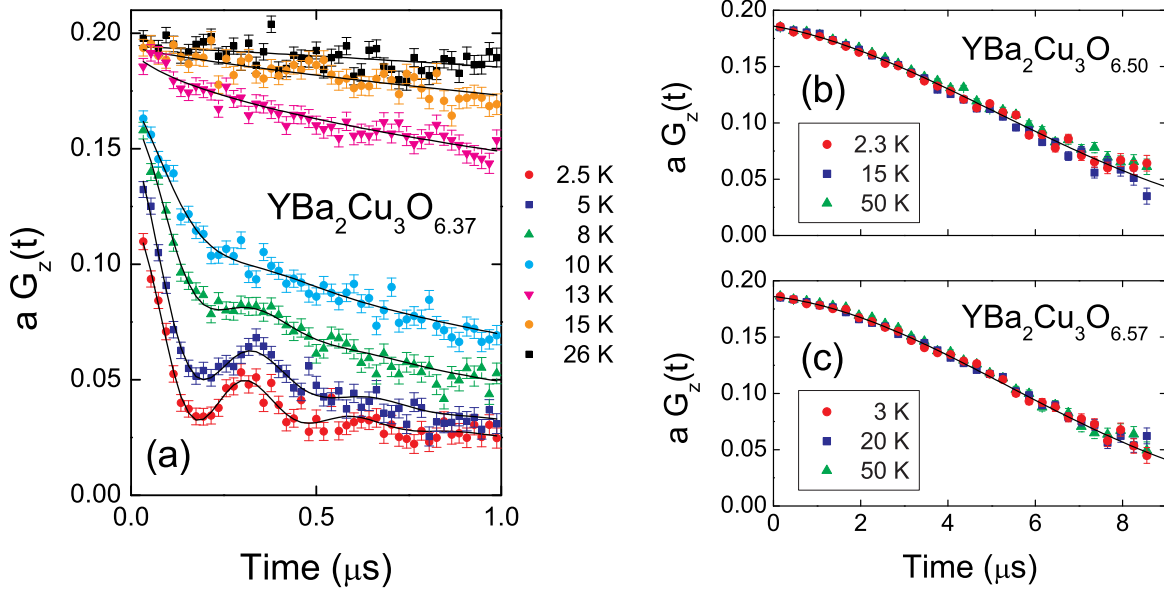


FIG. 16: Temperature dependence of the ZF- $\mu$ SR time signal for  $\text{YBa}_2\text{Cu}_3\text{O}_y$  single crystals recorded with the initial muon-spin polarization  $P(0)$  parallel to the  $\hat{c}$ -axis. The spectra for  $y=6.37$  come from the measurements of Ref. [130], whereas the spectra for  $y=6.50$  and  $y=6.57$  come from the work of Ref. [158]. The oscillations observed at low  $T$  for  $y=6.37$  indicate short-range magnetic order. The ZF- $\mu$ SR signals of  $y=6.50$  and  $y=6.57$  are identical, temperature-independent, and described by relaxation due to nuclear dipole moments and an additional weak exponential relaxation of unknown origin [127].

coexistence of stripe-like AF domains and superconducting material. The situation is in contrast to the coexistence of CSG magnetism and superconductivity observed in cation-substituted cuprates, which could be argued to be an extrinsic property arising from inherent disorder

[146]. Recent neutron scattering measurements by Stock *et al.* [147] on  $\text{YBa}_2\text{Cu}_3\text{O}_{6.353}$  single crystals support the occurrence of a single phase of coexisting superconductivity and short-range spin correlations. Fluctuating short-range commensurate spin correlations that develop

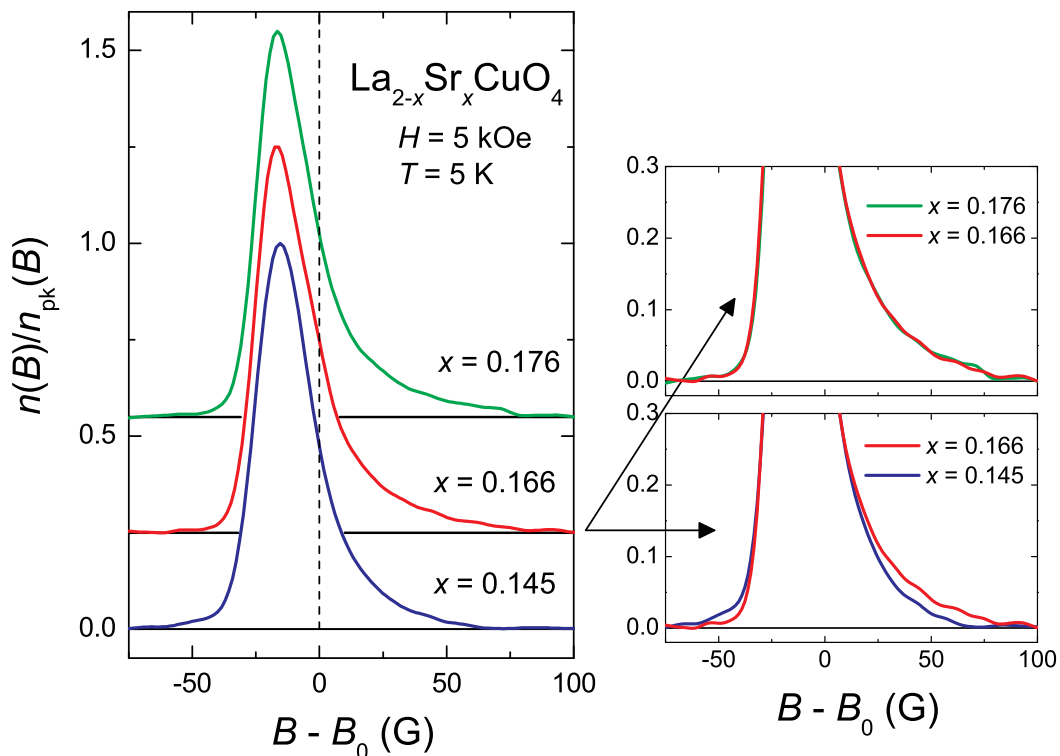


FIG. 17:  $\mu$ SR line shapes for  $\text{La}_{2-x}\text{Sr}_x\text{CuO}_4$  single crystals at  $H = 5$  kOe and  $T = 5$  K. For comparison, all line shapes have been normalized to their respective peak amplitude  $n_{\text{pk}}(B)$ . The dashed vertical line indicates the applied field  $B_0$ . The background signal from muons missing the sample and stopping elsewhere is very small, and hence there is no visible peak at  $B = B_0$ . The two panels on the right are blowups of the lower portion of the  $\mu$ SR line shapes, with the widths of the line shapes made equivalent to account for changes in  $\lambda_{ab}$ . The shape of  $n(B)$  clearly changes between  $0.145 < x < 0.166$ .

at temperatures well above  $T_c$  gradually slow down to form a spin glass-like state at low temperature. However, in contrast to the ZF- $\mu$ SR measurements, no transition to magnetic order of any kind is seen in the neutron measurements. Stock *et al.* have suggested that the magnetic freezing transition temperature observed in the ZF- $\mu$ SR experiments of Refs. [129, 130] is simply the temperature at which the slow spin dynamics observed by neutron scattering comes into the  $\mu$ SR time window. While this explanation is reasonable, it does not account for the oscillation observed in the ZF- $\mu$ SR signal at low  $T$ . A combined  $\mu$ SR and neutron scattering study on the same severely underdoped sample may reconcile this discrepancy.

#### Field-induced/enhanced magnetism

NMR experiments on near-optimally doped  $\text{YBa}_2\text{Cu}_3\text{O}_y$  [148, 149, 150],  $\text{YBa}_2\text{Cu}_4\text{O}_8$  [151] and  $\text{Tl}_2\text{Ba}_2\text{CuO}_{6+\delta}$  [152] have detected AF spin fluctuations in the vicinity of the vortex cores. Likewise, low-energy field-induced spin fluctuations have been detected by inelastic neutron scattering experiments on

$\text{La}_{1.837}\text{Sr}_{0.163}\text{CuO}_4$  [153]. As the fast spin fluctuation rates detected in these experiments fall outside the  $\mu$ SR time window, the field-induced spin dynamics in the high-doping regime cannot be studied by  $\mu$ SR. On the other hand, spin fluctuations slow down considerably in the low-doped regime and it is here where further information has recently been obtained by  $\mu$ SR.

#### $\text{La}_{2-x}\text{Sr}_x\text{CuO}_4$

There have been a couple of TF- $\mu$ SR studies providing evidence for frozen spins in the vortex cores of  $\text{La}_{2-x}\text{Sr}_x\text{CuO}_4$ . Kadono *et al.* [154] investigated the temperature dependence of the vortex core size at  $H = 2$  kOe in both underdoped and overdoped  $\text{La}_{2-x}\text{Sr}_x\text{CuO}_4$  single crystals. While the temperature dependence of the vortex core size at  $x = 0.19$  was found to be in qualitative agreement with the Kramer-Pesch effect, in the  $x = 0.13$  and  $x = 0.15$  samples the vortex core size increased with decreasing temperature and to a value significantly larger than expected from measurements of  $H_{c2}$ . The large size of the vortex cores in the lower doped samples was argued to result from a suppression of superconductivity around

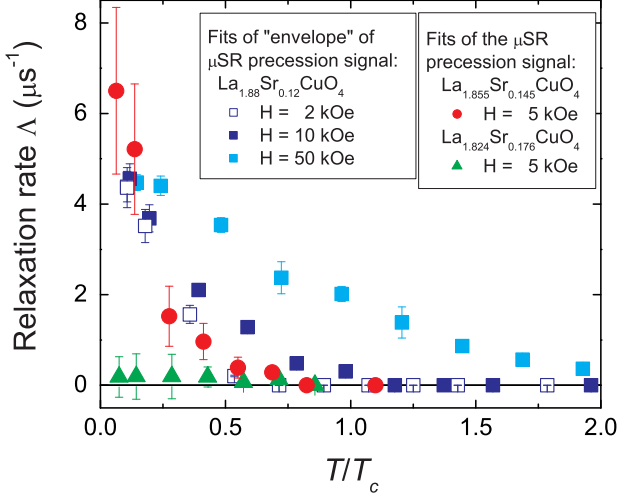


FIG. 18: Temperature dependence of the exponential relaxation rate  $\Lambda$  from fits of the TF- $\mu$ SR signal for  $\text{La}_{1.855}\text{Sr}_{0.145}\text{CuO}_4$  at  $H = 5$  kOe (circles) and  $\text{La}_{1.824}\text{Sr}_{0.176}\text{CuO}_4$  at  $H = 5$  kOe (triangles) to equation (23) [158]. Temperature dependence of the exponential relaxation rate  $\Lambda_1$  (squares) from fits of the ‘envelope’ of the TF- $\mu$ SR signal for  $\text{La}_{1.88}\text{Sr}_{0.12}\text{CuO}_4$  at  $H = 2$  kOe, 10 kOe and 50 kOe [161]. Note,  $\Lambda$  from Ref. [158] is associated with magnetism at the centre of the vortex core ( $r = 0$ ), where superconductivity is fully suppressed.

the vortex due to the formation of AF spin correlations. At the time, this seemed compatible with neutron experiments on  $\text{La}_{2-x}\text{Sr}_x\text{CuO}_4$  [155, 156] showing enhanced static AF spin correlations in underdoped samples. However, Kadono *et al.* speculated that the spin correlations responsible for the large vortex core size at low  $T$  and low  $H$  in  $\text{La}_{2-x}\text{Sr}_x\text{CuO}_4$  with  $x = 0.13$  and  $x = 0.15$  are not static, but dynamic. This interpretation was supported by a subsequent neutron study of an  $x = 0.144$  sample by Khaykovich *et al.* [157] that revealed static magnetic order only above  $H \approx 30$  kOe. However, not ruled out by these studies is the possibility that there is disordered static magnetism at low fields.

The latter possibility was considered in a more recent  $\mu$ SR study of  $\text{La}_{2-x}\text{Sr}_x\text{CuO}_4$  single crystals that are free of static magnetism in zero field [158]. Visually, evidence for static magnetism confined to the vortex cores can be seen in the TF- $\mu$ SR line shape as an unusual high-field ‘tail’ and the possible appearance of a low-field tail (depending on the magnitude and orientation of the fields in the vortex core), but with no other change in the shape of  $n(B)$ . As shown in figure 17, the high-field tail of the  $\mu$ SR line shape for  $\text{La}_{2-x}\text{Sr}_x\text{CuO}_4$  changes at a Sr doping  $0.145 \leq x \leq 0.166$ . However, similar changes of the  $\mu$ SR line shape could also arise from a 3D-to-2D crossover of the FLL. For example, in highly anisotropic  $\text{Bi}_{2+x}\text{Sr}_{2-x}\text{CaCu}_2\text{O}_{8+\delta}$  Lee *et al.* [159] showed that above a crossover field, random

pinning-induced misalignment of 2D ‘pancake’ vortices in adjacent layers narrows and reduces the asymmetry of the  $\mu$ SR line shape. For  $\text{La}_{2-x}\text{Sr}_x\text{CuO}_4$ , a similar scenario would imply that a reduction in Sr substitution significantly softens the flux lines and induces a degree of disorder sufficient to misalign the 2D vortices in adjacent layers. However, a combined  $\mu$ SR and neutron study of  $\text{La}_{1.90}\text{Sr}_{0.10}\text{CuO}_4$  by Divakar *et al.* [72] demonstrated that the vortices are 3D-like even at this lower Sr concentration. This conclusion is supported by neutron scattering experiments on  $\text{La}_{1.90}\text{Sr}_{0.10}\text{CuO}_4$  by Lake *et al.* [160], which show that the field-induced static magnetic order is 3D.

While the onset of magnetism is a more likely cause of the change in the  $\mu$ SR line shape of  $\text{La}_{2-x}\text{Sr}_x\text{CuO}_4$  with doping, the neutron study of Khaykovich *et al.* [157] implies that the line shape for  $x = 0.145$  measured at low  $T$  and low  $H$  in Ref. [158] does not result from static magnetic order. However, the TF- $\mu$ SR precession signals were found to be well described by the following polarization function, which allows for spin-glass like magnetism in and around the vortex cores

$$P(t) = \sum_i \exp(-\Lambda e^{-(r_i/\xi_{ab})^2} t) \cos[\gamma_\mu B(r_i)t]. \quad (23)$$

Here the sum is over all sites in the real-space unit cell of the FLL and  $B(r_i)$  is the local field at position  $r_i = (x_i, y_i)$  with respect to the vortex center. The distribution of fields at each site is assumed to be Lorentzian, and the relaxation rate  $\Lambda$  due to the magnetism is assumed to fall off as a function of radial distance from the vortex core centre on the scale of  $\xi_{ab}$ . The temperature dependences of  $\Lambda$  for  $\text{La}_{2-x}\text{Sr}_x\text{CuO}_4$  with  $x = 0.145$  and  $x = 0.16$  at  $H = 5$  kOe are shown in figure 18. The increase of  $\Lambda$  with decreasing temperature observed for the  $x = 0.145$  sample indicates a slowing down of spin fluctuations in the vortex-core region.

It is important to emphasize that these fits to the TF- $\mu$ SR time spectra don’t in themselves prove the existence of spin-glass order in the vortex cores. Other models based on different microscopic physics, including different forms of magnetism, may give equally good or better fits to the time-domain signals. The conclusion that magnetism occurs in the vortex cores really comes from the changes in the TF- $\mu$ SR line shape that are visually apparent as a function of temperature, magnetic field and hole doping. When the changes as a function of these three independent variables are considered together, there are really only two logical interpretations of the data. As already mentioned, experiments that have probed the dimensionality of the vortices in  $\text{La}_{2-x}\text{Sr}_x\text{CuO}_4$  more or less rule out the cause being a vortex transition. In the next section, experimental evidence that also argues against this being the interpretation for similar changes of the TF- $\mu$ SR line shape of  $\text{YBa}_2\text{Cu}_3\text{O}_y$  is discussed.

With this in mind, the results of the fits for

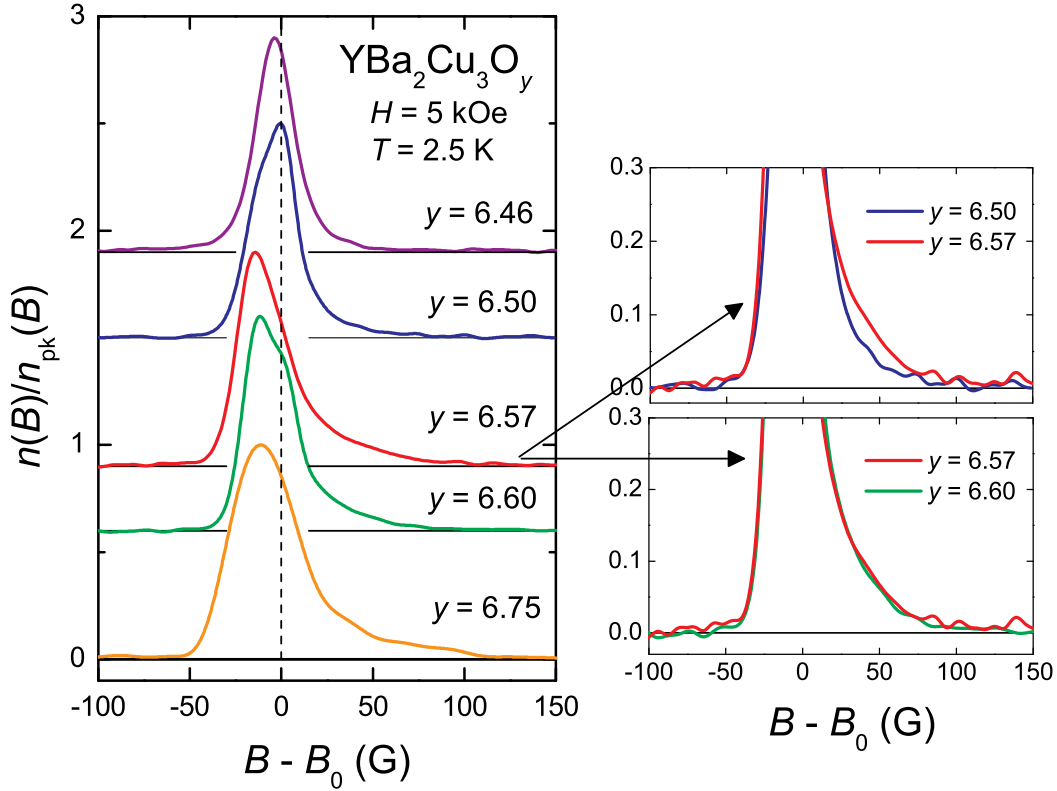
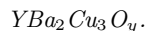


FIG. 19:  $\mu$ SR line shapes for  $\text{YBa}_2\text{Cu}_3\text{O}_y$  single crystals at  $H = 5$  kOe and  $T = 2.5$  K. For comparison, all line shapes have been normalized to their respective peak amplitude  $n_{\text{pk}}(B)$ . The dashed vertical line indicates the applied field  $B_0$ , and the bump or peak near this line (most visible for  $y = 6.50$ ) is the background signal. The two panels on the right show blowups of the lower portion of the  $\mu$ SR line shapes, with the widths of the line shapes made equivalent to account for changes in  $\lambda_{ab}$ . The shape of  $n(B)$  clearly changes between  $6.50 < y < 6.57$ .

$\text{La}_{1.855}\text{Sr}_{0.145}\text{CuO}_4$  may be compared to recent TF- $\mu$ SR measurements of  $\text{La}_{1.88}\text{Sr}_{0.12}\text{CuO}_4$  by Savici *et al.* [161], showing a field-induced enhancement of static or quasistatic magnetism. In contrast to the TF- $\mu$ SR studies discussed so far, information on field-induced magnetism was obtained in this work by fitting the ‘envelope’ of the muon spin precession signal at early times to a two-component exponential function  $E_1 \exp(-\Lambda_1 t) + E_2 \exp(-\Lambda_2 t)$ , where the first and second terms describe contributions to the  $\mu$ SR signal from volume fractions of the sample with and without quasistatic magnetism, respectively. This was possible for  $\text{La}_{1.88}\text{Sr}_{0.12}\text{CuO}_4$ , because the field-enhanced magnetism occupies a volume of the sample much larger than the volume of the vortex cores. In particular,  $E_1/E_2 > 60$  % compared to  $E_1/E_2 < 1$  %  $\text{La}_{1.855}\text{Sr}_{0.145}\text{CuO}_4$  in Ref. [158]. As shown in figure 18, the temperature dependence of the relaxation rate  $\Lambda$  of  $\text{La}_{1.855}\text{Sr}_{0.145}\text{CuO}_4$  determined from fits of the full TF- $\mu$ SR precession signal with equation (23) is similar to the temperature dependence of the relaxation rate  $\Lambda_1$  determined from fits to the envelope function of  $\text{La}_{1.88}\text{Sr}_{0.12}\text{CuO}_4$  at low  $H$ . This seems to suggest that the static (or quasistatic) magnetism that occurs in a large volume of  $\text{La}_{1.88}\text{Sr}_{0.12}\text{CuO}_4$  in a magnetic field is

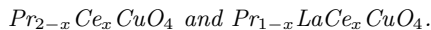
similar to the magnetism found near the vortex cores in  $\text{La}_{1.855}\text{Sr}_{0.145}\text{CuO}_4$ . However, this is unlikely the case at low temperatures. In contrast to  $\text{La}_{1.855}\text{Sr}_{0.145}\text{CuO}_4$ , static magnetic correlations occur in  $\text{La}_{1.88}\text{Sr}_{0.12}\text{CuO}_4$  even in zero field [156]. Thus the fast relaxation rate observed in  $\text{La}_{1.88}\text{Sr}_{0.12}\text{CuO}_4$  in the vortex state at low  $T$  can be attributed to static magnetic order.

The study by Savici *et al.* also showed that quasistatic magnetism persists to temperatures well above  $T_c$  at high  $H$ . This implies that vortices are not required to nucleate static magnetism in superconducting samples. Instead the vortices act to suppress spin fluctuations and enhance the magnetic volume fraction. The TF- $\mu$ SR experiments by Savici *et al.* [161] provide strong evidence for these effects, as well as neutron scattering experiments on  $\text{La}_{1.88}\text{Sr}_{0.12}\text{CuO}_4$  by Katano *et al.* [156] showing field-enhanced AF spin correlations at  $H = 100$  kOe and low  $T$ , and Raman scattering experiments on  $\text{La}_{1.88}\text{Sr}_{0.12}\text{CuO}_4$  by Machtoub *et al.* [162] that can be explained in terms of a field-enhanced AF volume fraction.



Miller *et al.* [163] reported evidence from TF- $\mu$ SR measurements on  $\text{YBa}_2\text{Cu}_3\text{O}_{6.50}$  at  $H \geq 10$  kOe for the occurrence of static AF order in the vortex cores. While Kadono *et al.* [167] were able to fit low field TF- $\mu$ SR spectra for underdoped  $\text{La}_{2-x}\text{Sr}_x\text{CuO}_4$  assuming the spatial field profile  $B(\mathbf{r})$  of the FLL is adequately described by the London model with a Lorentzian cutoff factor  $F(G) = \exp(-\sqrt{2}G\xi)$ , fits of the  $\mu$ SR time spectra for  $\text{YBa}_2\text{Cu}_3\text{O}_{6.50}$  assuming a conventional London or GL model were found not to converge. In Ref. [163] the TF- $\mu$ SR signal from  $\text{YBa}_2\text{Cu}_3\text{O}_{6.50}$  could be fit assuming static AF order in the vortex cores commensurate with the underlying crystal lattice, even though to date field-induced static magnetic order has not been detected in  $\text{YBa}_2\text{Cu}_3\text{O}_y$  by neutron scattering. The magnitude of the staggered field sensed at the *muon stopping site(s)* was determined to be  $\sim 18$  G at low  $T$ . However, this analysis still required the value of  $\xi_{ab}$  to be constrained, which suggests an insensitivity to the high-field tail of the  $\mu$ SR line shape or that the assumed theoretical model is inappropriate.

Recently, the doping, temperature and magnetic field dependences of the  $\mu$ SR line shape for  $\text{YBa}_2\text{Cu}_3\text{O}_y$  single crystals were studied in some detail [158].  $\mu$ SR line shapes for  $\text{YBa}_2\text{Cu}_3\text{O}_{6.46}$  and  $\text{YBa}_2\text{Cu}_3\text{O}_{6.50}$  were found to be compatible with spin-glass magnetism appearing in and around the vortex cores (some of these measurements are shown in figure 19). This interpretation of the  $\mu$ SR signal explains why frozen spins have not been detected in the vortex cores of  $\text{YBa}_2\text{Cu}_3\text{O}_y$  by neutron scattering, which is insensitive to static magnetism with random spatial correlations. As in the case of  $\text{La}_{2-x}\text{Sr}_x\text{CuO}_4$ , an explanation of the observed changes in the TF- $\mu$ SR line shape in terms of a crossover in the dimensionality of the vortices is unlikely. Josephson plasma resonance measurements by Dulic *et al.* [80] indicate that the vortices in  $\text{YBa}_2\text{Cu}_3\text{O}_{6.50}$  are 3D-like at low temperatures. Consistent with this finding, mutual inductance measurements show that even severely underdoped  $\text{YBa}_2\text{Cu}_3\text{O}_y$  becomes quasi-2D only near  $T_c$  [30].



The first reported experimental evidence for field-induced magnetic order in an electron-doped cuprate superconductor came from a TF- $\mu$ SR study of underdoped  $\text{Pr}_{2-x}\text{Ce}_x\text{CuO}_4$  single crystals [164]. In zero field, random magnetism was detected, but a remarkably weak applied field of only 90 Oe resulted in the occurrence of static AF order throughout the volume of the sample. The onset of bulk AF order below  $T_c$  is visually apparent from the observed positive field-shift of the *entire*  $\mu$ SR line shape (see figure 20). In this case, the entire line

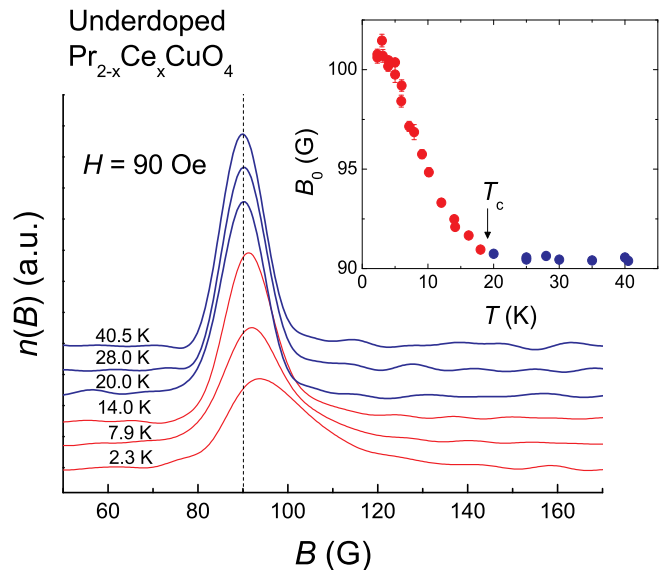


FIG. 20: Temperature dependence of the  $\mu$ SR line shape in an underdoped  $\text{Pr}_{2-x}\text{Ce}_x\text{CuO}_4$  single crystal at  $H = 90$  Oe [164]. Inset: Temperature dependence of the average internal magnetic field  $B_0$ . The blue and red colour scheme denotes measurements taken above and below  $T_c$ , respectively.

shape shifts to higher  $B$  because the AF order enhances the local magnetic field at all of the O(3) muon stopping sites.

The occurrence of weak field-induced AF order was subsequently identified in superconducting  $\text{Pr}_{1-x}\text{LaCe}_x\text{CuO}_4$  with  $x=0.11$  and  $x=0.15$ , in TF- $\mu$ SR studies by Kadono *et al.* [166, 167]. In these experiments it was argued that the muon senses the antiferromagnetism indirectly through a transferred hyperfine coupling between the  $\mu^+$  spin and the Cu moments via the Pr ions, rather than by direct detection of the dipolar fields of the Cu moments at the muon site as suggested in Ref. [164, 165].

Single crystals of  $\text{Pr}_{1-x}\text{LaCe}_x\text{CuO}_4$  can be made much larger than single crystals of  $\text{Pr}_{2-x}\text{Ce}_x\text{CuO}_4$ , and this has allowed neutron scattering studies of this compound. Fujita *et al.* used neutrons to study the same  $\text{Pr}_{1-x}\text{LaCe}_x\text{CuO}_4$  samples that Kadono *et al.* investigated with  $\mu$ SR [168]. In zero field, weak AF order was detected in the  $x = 0.11$  sample, in contrast to ZF- $\mu$ SR measurements that found only random magnetism due to small Pr moments [169]. This apparent discrepancy suggests that the AF correlations in zero field are fluctuating on the  $\mu$ SR time scale. The neutron experiments by Fujita *et al.* also demonstrated a field-induced enhancement of AF order in the  $x = 0.11$  sample, whereas static AF order was not observed at all in the  $x = 0.15$  sample. The latter result contrasts the TF- $\mu$ SR experiments of Kadono *et al.* who reported field-induced AF order in the  $x = 0.15$  sample, but with a reduced ordered

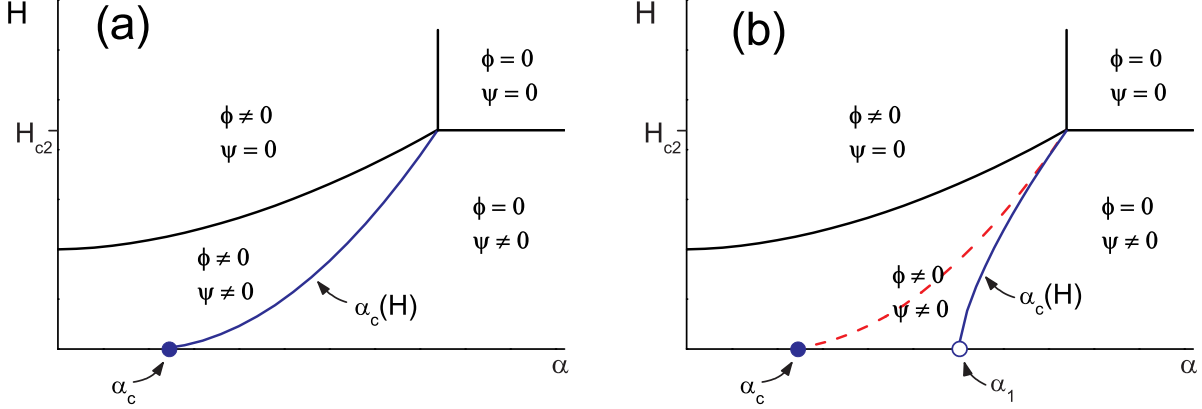


FIG. 21: Schematic of theoretically predicted zero-temperature phase diagrams for (a) 2D vortices (adapted from figure 1 of Ref. [171]), and (b) 3D vortices (adapted from figure 1 of Ref. [173]). Here  $\alpha$  is a control parameter (*e.g.* carrier concentration).  $\Psi$  and  $\phi$  denote the expectation values of the superconducting and competing order parameters, respectively. The solid blue curve represents a quantum phase transition (QPT) and the solid blue dot denoted  $\alpha_c$  is a quantum critical point (QCP). Note that the QPT for the 2D vortex case is a crossover within the coexistence phase of the 3D vortex phase diagram (red dashed curve). Below the crossover curve, the competing order is spatially inhomogeneous. In addition, the zero field extrapolation of the QPT in (b) is an ‘avoided’ QCP (open blue circle).

local moment. More recently, Kang *et al.* have detected static SDW order and residual AF order in underdoped  $\text{Pr}_{1-x}\text{LaCe}_x\text{CuO}_4$  at zero field by neutron scattering, but not in optimally doped  $\text{Pr}_{1-x}\text{LaCe}_x\text{CuO}_4$  [170]. Furthermore, they showed that a  $\hat{c}$ -axis aligned magnetic field enhances the SDW order, but not the AF order in underdoped  $\text{Pr}_{1-x}\text{LaCe}_x\text{CuO}_4$ , and does not induce static magnetic order of either kind in optimally doped  $\text{Pr}_{1-x}\text{LaCe}_x\text{CuO}_4$ .

### Piecing together the information from $\mu\text{SR}$

ZF- $\mu\text{SR}$  and TF- $\mu\text{SR}$  studies of cuprates have established that superconductivity and static (quasistatic) magnetism coexist on the low-doping side of the superconducting ‘dome’. In quality samples, this coexistence is on a nanometer scale at zero magnetic field. *Field-induced* static magnetism has been detected at low temperatures in samples where the spin fluctuation rate at  $H = 0$  falls outside the  $\mu\text{SR}$  time window. In these samples, disordered static magnetism is induced by weak magnetic fields.

As discussed in Ref. [140], neutron scattering studies of  $\text{La}_{2-x}\text{Sr}_x\text{CuO}_4$  and  $\text{La}_2\text{CuO}_{4+y}$  support a theoretical model of competing superconducting and magnetic order parameters proposed by Demler *et al.* [171]. In this model the pure superconductor undergoes a field-dependent quantum phase transition (QPT) to a state of coexisting superconductivity and magnetic order (see figure 21a). The competing magnetic order is stabilized at the QPT by the suppression of superconductivity associ-

ated with the formation of vortices. In agreement with the theory, the neutron experiments have detected *field-induced* magnetic order [157] and have shown that the ordered magnetic moment grows with increasing magnetic field exactly as predicted [155, 174]. The theoretical model of Demler *et al.* is not exclusive to the cuprates, as it also appears to describe the occurrence of a field-induced coexistence phase of magnetic order and superconductivity in  $\text{CeRhIn}_5$  [172].

In actuality the theoretical model of Demler *et al.* is somewhat oversimplified. In particular, the model assumes that the vortices are 2D. As a finite size system, an isolated 2D vortex cannot support static magnetic order. It is only when the 2D vortices strongly couple to their neighbours is static magnetic order stabilized. Thus the coexistence phase in the theory of Demler *et al.* is characterized by a competing order parameter that is nearly spatially uniform throughout the sample. However, as mentioned earlier, neutron scattering studies of  $\text{La}_{1.90}\text{Sr}_{0.10}\text{CuO}_4$  by Lake *et al.* [160] show that the magnetic order in the vortex state is in fact 3D. As explained in Ref. [160], this implies that there is significant coupling between the  $\text{CuO}_2$  planes, so that the vortices themselves are 3D. As discussed earlier, this same conclusion was reached in a TF- $\mu\text{SR}$  study of  $\text{La}_{1.90}\text{Sr}_{0.10}\text{CuO}_4$  by Divakar *et al.* [72].

Kivelson *et al.* [173] have extended the theory of Demler *et al.* to account for the coupling between  $\text{CuO}_2$  layers, and showed that in contrast to an isolated 2D vortex, a competing order parameter could be stabilized in an isolated 3D vortex line. This leads to a modification of the phase diagram proposed by Demler *et al.*,



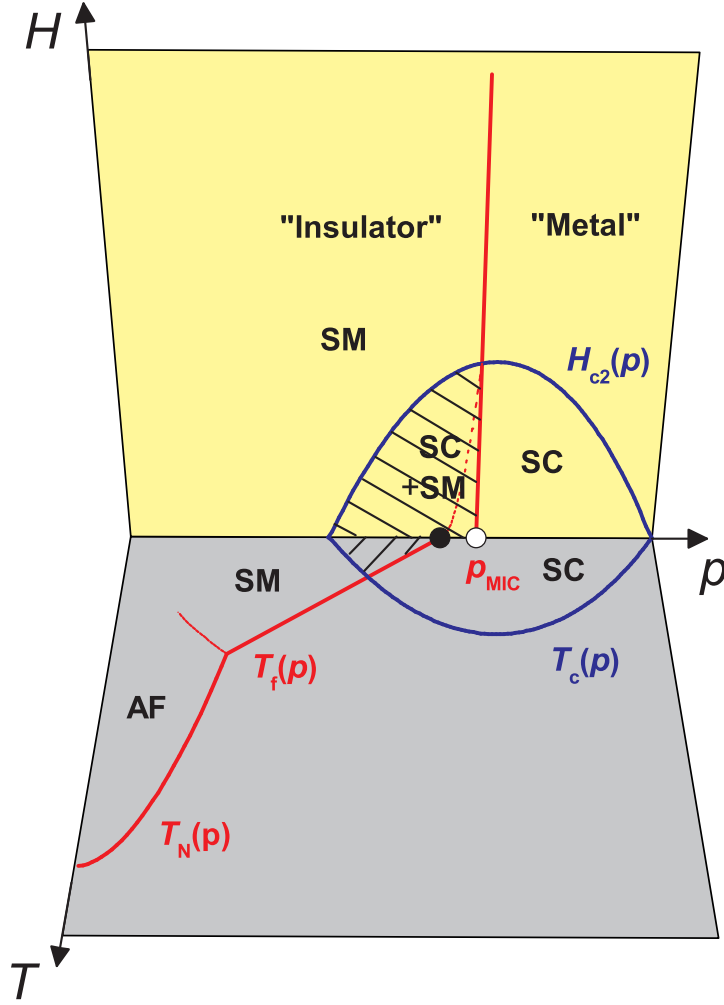


FIG. 22: Generic phase diagram inferred from  $\mu$ SR studies on high- $T_c$  superconductors. The acronyms for the different phases are defined as follows: **AF**  $\equiv$  antiferromagnetic phase, **SM**  $\equiv$  static magnetic phase (where magnetism may be disordered), **SC**  $\equiv$  superconducting phase, and **SC + SM**  $\equiv$  coexisting superconducting and static magnetic phases.  $T_c(p)$ ,  $T_N(p)$ ,  $T_f(p)$ ,  $H_{c2}(p)$  and  $p_{\text{MIC}}$  denote the superconducting critical temperature, the Neel temperature, the spin freezing temperature, the upper critical magnetic field and the  $T \rightarrow 0$  metal-to-insulator crossover (MIC), respectively. TF- $\mu$ SR measurements indicate that the crossover at  $p_{\text{MIC}}$  extends below  $H_{c2}(p)$ , separating a superconducting phase with fast spin fluctuations from a superconducting phase that coexists with static magnetism. ZF- $\mu$ SR measurements indicate that superconductivity and static magnetism coexist on a nanometer scale at  $H=0$ , but only up to a carrier concentration  $p$  that is less than  $p_{\text{MIC}}$ . Above the dashed red curve, the static magnetism is uniformly distributed throughout the sample.

such that the *true* QPT is to a phase in which a spatially inhomogeneous competing order coexists with superconductivity (see figure 21b). The TF- $\mu$ SR experiments on  $\text{La}_{2-x}\text{Sr}_x\text{CuO}_4$  ( $0.12 < x < 0.166$ ) [154, 158] and  $\text{YBa}_2\text{Cu}_3\text{O}_y$  ( $y < 6.57$ ) [158, 163] strongly support the existence of this phase. The observed changes in the  $\mu$ SR line shape are consistent with the onset of *disordered* static magnetism in and around weakly interacting vortices. These experiments imply that the competing order parameter stabilized at the QPT is the mean squared *local* magnetization. With increasing magnetic field, stronger overlap of the magnetism around

neighbouring vortices may lead to a co-operative bulk crossover to long-range magnetic order, as is apparently the case in  $\text{La}_{1.856}\text{Sr}_{0.144}\text{CuO}_4$  [157]. However, so far this has not been observed in  $\text{YBa}_2\text{Cu}_3\text{O}_y$  where the QPT identified by  $\mu$ SR is closer to the low-doping side of the superconducting ‘dome’. While the QPT in electron-doped cuprates has not been accurately determined by  $\mu$ SR or neutron scattering, experiments to date suggest the coexistence phase is dominated by static magnetic order rather than disordered static magnetism—likely due to close proximity of the AF and superconducting phases.

The TF- $\mu$ SR experiments on  $\text{La}_{2-x}\text{Sr}_x\text{CuO}_4$  and

YBa<sub>2</sub>Cu<sub>3</sub>O<sub>y</sub> of Ref. [158] indicate that the QPT in figure 21b occurs at the critical doping below which the temperature dependence of the normal-state resistivity  $\rho$  at  $H > H_{c2}$  and low- $T$  changes from *metallic* behaviour ( $d\rho/dT > 0$ ) to an unusual *insulating* behaviour ( $d\rho/dT < 0$ ) [175, 176, 177, 178, 179, 180]. This low-temperature metal-to-insulator (MIC) crossover has also been detected indirectly by thermal conductivity measurements as a function of magnetic field [181, 182, 183]. Although the MIC is a generic property of high- $T_c$  cuprates, it occurs at a non-universal carrier concentration. The onset of static magnetism below the MIC detected by TF- $\mu$ SR is compatible with the localization of charge. In zero-field, deviations from a linear dependence of the resistivity on  $T$  are observed in underdoped samples, including upturns of the resistivity with decreasing temperature in very underdoped superconducting samples. Theoretically, Marchetti *et al.* [184, 185] have argued that the cause of the MIC in both zero field and strong magnetic fields is the same, and is due to the onset of short-range AF order [184]. This seems compatible with the ZF- $\mu$ SR studies that have detected static magnetism in underdoped samples.

A key prediction of the theory of Ref. [173] is that there is an ‘avoided’ QCP at  $H=0$ . In other words, the QCP lies at a lower doping than one expects from the extrapolated  $H \rightarrow 0$  location of the QPT at finite magnetic field. In La<sub>2-x</sub>Sr<sub>x</sub>CuO<sub>4</sub>, the spin freezing transition temperature  $T_g$  at  $H=0$  deduced from ZF- $\mu$ SR [125, 126] and NQR [138] experiments extrapolates to zero below the critical doping for the MIC at  $x \approx 0.16$  [175, 181, 182] (see figure 15). The same is true for YBa<sub>2</sub>Cu<sub>3</sub>O<sub>y</sub>, where static magnetism associated with Cu spins is not observed by ZF- $\mu$ SR [122, 129, 158, 163] in samples immediately below the critical doping for the MIC at  $y \approx 6.55$  [183].

Figure 22 shows the generic magnetic phase diagram suggested by ZF- $\mu$ SR and TF- $\mu$ SR experiments on cuprates. In this figure the QCP and ‘avoided’ QCP are shown as solid and open circles, respectively. Note that the zero-field QCP here is distinct from the universal QCP near  $p = 0.19$  that has been suggested by Tallon and others [126, 186, 188]. In other words, there may in fact be two unrelated quantum critical points under the superconducting ‘dome’ that strongly influence the physical properties of a large portion of the cuprate phase diagram. While neutron scattering and  $\mu$ SR measurements both support a generic phase diagram ruled by the close competition between superconducting and magnetic orders, it is still to be determined whether *some* magnetism is also responsible for the ‘glue’ that binds the superconducting carriers.

## Acknowledgments

The work presented here was supported by the Natural Science and Engineering Research Council of Canada, and the Quantum Materials program of the Canadian Institute for Advanced Research.

## References

- 
- \* Electronic address: jsonier@sfu.ca
- [1] Sonier J E, Brewer J H and Kiefl R F 2000 *Rev. Mod. Phys.* **72** 769
  - [2] Herlach D *et al.* 1990 *Hyperfine Interactions* **63** 41
  - [3] Sonier J E *et al.* 1997 *Phys. Rev. Lett.* **79** 1742
  - [4] Golubov A A and Hartmann U 1994 *Phys. Rev. Lett.* **72** 3602
  - [5] Kirtley J R, Kogan V G, Clem J R and Moler K A 1999 *Phys. Rev. B* **59** 4343
  - [6] Niedermayer Ch *et al.* 1999 *Phys. Rev. Lett.* **83** 3932
  - [7] Morenzoni E, Prokscha T, Suter A, Luetkens H and Khasanov R 2004 *J. Phys.: Condens. Matter* **16** S4583
  - [8] Salman Z *et al.* 2007 *Phys. Rev. Lett.* **98** 167001
  - [9] Dawson W K, Tibbs K, Weathersby S P, Boekema C and Chan K-C B 1988 *J. Appl. Phys.* **64** 5809
  - [10] Brewer J H *et al.* 1990 *Hyperfine Interactions* **63** 177
  - [11] Schneider J W *et al.* 1993 *Phys. Rev. Lett.* **71** 557
  - [12] Chakhalian J A *et al.* 1997 *Hyperfine Interactions* **106** 245
  - [13] Brandt E H 1988 *Phys. Rev. B* **37** 2349(R)
  - [14] Brandt E H 1991 *Phys. Rev. Lett.* **66** 3213
  - [15] Yaouanc A *et al.* 1998 *J. Phys.: Condens. Matter* **10** 9791
  - [16] Barford W and Gunn J M F 1988 *Physica C* **156** 515
  - [17] Harshman D R *et al.* 1987 *Phys. Rev. B* **36** 2386(R)
  - [18] Uemura Y J *et al.* 1988 *Phys. Rev. B* **38** 909(R)
  - [19] Harshman D R *et al.* 1989 *Phys. Rev. B* **39** 851(R)
  - [20] Pümpin B *et al.* 1990 *Phys. Rev. B* **42** 8019
  - [21] Uemura Y J *et al.* 1989 *Phys. Rev. Lett.* **62** 2317
  - [22] Uemura Y J *et al.* 1991 *Phys. Rev. Lett.* **66** 2665
  - [23] Yaouanc A, Dalmas de Réotier P and Brandt E H 1997 *Phys. Rev. B* **55** 11107
  - [24] Ando Y and Segawa K 2002 *Phys. Rev. Lett.* **88** 167005
  - [25] Wen H H *et al.* 2003 *Europhys. Lett.* **64** 790
  - [26] Wang Y *et al.* 2003 *Science* **299** 86
  - [27] Brandt E H 2003 *Phys. Rev. B* **68** 054506
  - [28] Celio M, Riseman T M, Kiefl R F, Brewer J H and Kossler W J 1988 *Physica C* **153-155** 753
  - [29] Pereg-Barnea T *et al.* 2004 *Phys. Rev. B* **69** 184513
  - [30] Zuev Y, Kim M S and Lemberger T R 2005 *Phys. Rev. Lett.* **95** 137002
  - [31] Broun D M *et al.* 2007 *Phys. Rev. Lett.* **99** 237003
  - [32] Tallon J L, Loram J W, Cooper J R, Panagopoulos C and Bernhard C 2003 *Phys. Rev. B* **68** 180501(R)
  - [33] Hardy W N *et al.* 1993 *Phys. Rev. Lett.* **70** 3999
  - [34] Sonier J E *et al.* 1994 *Phys. Rev. Lett.* **72** 744
  - [35] Luke G M *et al.* 1997 *Physica C* **282-287** 1465
  - [36] Van Harlingen D J 1995 *Rev. Mod. Phys.* **67** 515

- [37] Amin M H S, Franz M and Affleck I 1998 Phys. Rev. B **58** 5848
- [38] Sonier J E *et al.* 1999 Phys. Rev. Lett. **83** 4156
- [39] Amin M H S, Franz M and Affleck I 2000 Phys. Rev. Lett. **84** 5864
- [40] Sonier J E 2004 *J. Phys.:Condens. Matter* **16** S4499
- [41] Callaghan F D, Laulajainen M, Kaiser C V and Sonier J E 2005 Phys. Rev. Lett. **95** 197001
- [42] Laulajainen M, Callaghan F D, Kaiser C V and Sonier J E 2006 Phys. Rev. B **74** 054511
- [43] Laiho R, Safonchik M and Taito K B 2006 Phys. Rev. B **73** 024507
- [44] Laiho R, Safonchik M and Taito K B 2007 Phys. Rev. B **75** 174524
- [45] Landau I L and Keller H *arXiv:0704.1268v2*
- [46] Brandt E H 1977 *J. Low Temp. Phys.* B **24** 709
- [47] Brandt E H 1988 *J. Low Temp. Phys.* B **73** 355
- [48] Brandt E H 1992 *Physica C* **195** 1
- [49] de Oliveira I G and Thompson A M 1998 Phys. Rev. B **57** 7477
- [50] Laiho R, Lähderanta E, Safonchik M and Taito K B 2005 Phys. Rev. B **71** 024521
- [51] Riseman T M *et al.* 1995 Phys. Rev. B **52**, 10569
- [52] Sonier J E *et al.* 1997 Phys. Rev. B **55** 11789
- [53] Kadono R *et al.* 2001 Phys. Rev. B **63** 224520
- [54] Ohishi K *et al.* 2002 Phys. Rev. B **65** 140505
- [55] Price A N *et al.* 2002 Phys. Rev. B **65** 214520
- [56] Clem J R 1975 *J. Low Temp. Phys.* **18** 427
- [57] Brandt E H 1997 Phys. Rev. Lett. **78** 2208
- [58] Takanaka K 1971 *Prog. Theor. Phys.* **46** 1301
- [59] Ichioka M, Hayashi N, Enomoto N and Machida K 1996 Phys. Rev. B **53** 15316
- [60] Kogan V G *et al.* 1997 Phys. Rev. B **55** R8693
- [61] Kogan V G, Miranović P, Dobrosavljević-Grujić Lj, Pickett W E and Christen D K 1997 Phys. Rev. Lett. **79** 741
- [62] Nakai N, Miranović P, Ichioka M and Machida K 2002 Phys. Rev. Lett. **89** 237004
- [63] Luke G M *et al.* 2000 *Physica B* **289** 373
- [64] Sonier J E *et al.* 2004 Phys. Rev. Lett. **93** 017002
- [65] Kadono K *et al.* 2006 Phys. Rev. B **74** 024513
- [66] Affleck I, Franz M and Amin M H 1996 Phys. Rev. B **55** R704
- [67] Agterberg D F 1998 Phys. Rev. B **58** 14484
- [68] Heeb R and Agterberg D F 1999 Phys. Rev. B **59** 7076
- [69] Sosolik C E *et al.* 2003 Phys. Rev. B **68** 140503(R)
- [70] Giamarchi T and Le Doussal P 1995 Phys. Rev. B **52** 1242
- [71] Dalmas de Réotier P, Gubbens P C M and Yaouanc A 2004 *J. Phys.:Condens. Matter* **16** S4687
- [72] Divakar U *et al.* 2004 Phys. Rev. Lett. **92** 237004
- [73] Menon G I *et al.* 2006 Phys. Rev. Lett. **97** 177004
- [74] Koshelev A E, Glazman L I and Larkin A I 1996 Phys. Rev. B **53**, 2786
- [75] Menon G I *et al.* 1999 Phys. Rev. B **60** 7207
- [76] Harshman D R *et al.* 1993 Phys. Rev. B **47** 2905
- [77] Harshman D R *et al.* 2004 Phys. Rev. B **69** 174505
- [78] Deak J, Hou L, Metcalf P and McElfresh M 1995 *Phys. Rev. B* **51** 705(R)
- [79] Sefrioui Z *et al.* 1999 Phys. Rev. B **60** 15423
- [80] Dulić D *et al.* 2001 Phys. Rev. Lett. **86**, 4660
- [81] Ichioka M, Hasegawa A and Machida K 1999 Phys. Rev. B **59** 184
- [82] Ichioka M, Hasegawa A and Machida K 1999 Phys. Rev. B **59** 8902
- [83] Caroli C, de Gennes P G and Matricon J 1964 *Phys. Lett.* **9** 307
- [84] Pöttinger B and Klein U 1993 Phys. Rev. Lett. **70** 2806
- [85] Dukan S and Tesanović Z 1994 Phys. Rev. B **49** 13017
- [86] Tesanović Z and Sacramento P 1998 Phys. Rev. Lett. **80** 1521 8902
- [87] Kogan V G and Zhelezina N V 2004 Phys. Rev. B **71** 134505
- [88] DeBeer-Schmitt L, Dewhurst C D, Hoogenboom B W, Petrovic C and Eskildsen M R 2006 Phys. Rev. Lett. **97** 127001
- [89] Nakai N, Miranović P, Ichioka M and Machida K 2006 Phys. Rev. B **73** 172501
- [90] Parks R D (ed) 1969 in *Superconductivity* vol 2 (New York: Marcel Dekker Inc.) p 817
- [91] Volovik G E 1993 *JETP Lett.* **58** 469
- [92] Sonier J E, Hundley M F, Thompson J D and Brill J W 1999 Phys. Rev. Lett. **82** 4914
- [93] Nakai N, Miranović P, Ichioka M and Machida K 2004 Phys. Rev. B **70** 100503
- [94] Sonier J E, Hundley M F and Thompson J D 2006 Phys. Rev. B **73** 132504
- [95] Boaknin E *et al.* 2001 Phys. Rev. Lett. **87** 237001
- [96] Chiao M, Hill R W, Lupien C, Popic B, Gagnon R and Taillefer L 1999 Phys. Rev. Lett. **82** 2943
- [97] Kübert C and Hirschfeld P J 1998 Phys. Rev. Lett. **80** 4963
- [98] Vekhter I and Houghton A 1999 Phys. Rev. Lett. **83** 4626
- [99] Boaknin E *et al.* 2003 Phys. Rev. Lett. **90** 117003
- [100] Lowell J and Sousa J B 1970 *J. Low Temp. Phys.* **3** 65
- [101] Yokoya T *et al.* 2001 *Science* **294** 2518
- [102] Rodrigo J G and Vieira S 2004 *Physica C* **404** 306
- [103] Fletcher J D *et al.* 2007 Phys. Rev. Lett. **75** 045019
- [104] Nakai N, Ichioka M and Machida K 2002 *J. Phys. Soc. Jpn.* **71** 23
- [105] Koshelev A E and Golubov A A 2003 Phys. Rev. Lett. **90** 177002
- [106] Dahm T, Graser S and Schopohl N 2004 *Physica C* **408-410** 336
- [107] Ichioka M, Machida K, Nakai N and Miranović P 2004 Phys. Rev. B **70** 144508
- [108] Eskildsen M R *et al.* 2002 Phys. Rev. Lett. **89** 187003
- [109] Klein T, Lyard L, Marcus J, Holanava Z and Marcenat C 2006 Phys. Rev. B **73** 184513
- [110] Sologubenko A V, Jun J, Kazakov S M, Karpinski J and Ott H R 2002 Phys. Rev. B **66** 014504
- [111] Seyfarth G *et al.* 2005 Phys. Rev. Lett. **95** 107004
- [112] Seyfarth G *et al.* 2006 Phys. Rev. Lett. **97** 236403
- [113] Atkinson W A, private communication.
- [114] Brown S P *et al.* 2004 Phys. Rev. Lett. **92** 067004
- [115] Hill R W *et al.* 2004 Phys. Rev. Lett. **92** 027001
- [116] Shulga S V *et al.* 1998 Phys. Rev. Lett. **80** 1730
- [117] Doh H, Sigrist M, Cho B K and Lee S -I 1999 Phys. Rev. Lett. **83** 5350
- [118] Mukhopadhyay S, Sheet G, Raychaudhuri P and Takeya H 2005 Phys. Rev. B **72** 014545
- [119] Huang C L *et al.* 2006 Phys. Rev. B **73** 012502
- [120] Nakagawa H, Takamasu T, Miura N and Enomoto Y 1998 *Physica B* **246-247** 429
- [121] Kadono R 2004 *J. Phys.:Condens. Matter* **16** S4421
- [122] Kiefl R F *et al.* 1989 Phys. Rev. Lett. **63** 2136
- [123] Weidinger A *et al.* 1989 Phys. Rev. Lett. **62** 102

- [124] Heffner R H and Cox D L 1989 Phys. Rev. Lett. **63** 2538
- [125] Niedermayer Ch *et al.* 1998 Phys. Rev. Lett. **80** 3843
- [126] Panagopoulos C *et al.* 2002 Phys. Rev. B **66** 064501
- [127] Sonier J E *et al.* 2001 *Science* **292** 1692
- [128] Kanigel A *et al.* 2002 Phys. Rev. Lett. **88** 137003
- [129] Sanna S, Allodi G, Concas G, Hillier A D and De Renzi R 2004 Phys. Rev. Lett. **93** 207001
- [130] Miller R I *et al.* 2006 Phys. Rev. B **73** 144509
- [131] Basov D N *et al.* 1995 Phys. Rev. Lett. **74** 598
- [132] Lee Y-S, Segawa K, Ando Y and Basov D N 2005 Phys. Rev. Lett. **94** 137004
- [133] Atkinson W A and Carbotte J P 1995 Phys. Rev. B **52** 10601
- [134] Xiang T and Wheatley J M 1996 Phys. Rev. Lett. **76** 134
- [135] Grévin B, Berthier Y and Collin G 2000 Phys. Rev. Lett. **85** 1310
- [136] Sonier J E *et al.* 2002 Phys. Rev. B **66** 134501
- [137] Cho J H, Borsa F, Johnston D C and Torgeson D R 1992 Phys. Rev. B **46** 3179
- [138] Chou F C *et al.* 1993 Phys. Rev. Lett. **71** 2323
- [139] Julien M -H *et al.* 1999 Phys. Rev. Lett. **83** 604
- [140] Birgeneau R J, Stock C, Tranquada J M and Yamada K 2006 J. Phys. Soc. Jpn. **75** 111003
- [141] Wakimoto S *et al.* 1999 Phys. Rev. B **60** R769
- [142] Matsuda M *et al.* 2000 Phys. Rev. B **62** 9148
- [143] Wakimoto S *et al.* 2001 Phys. Rev. B **63** 172501
- [144] Shraiman B I and Siggia E D 1989 Phys. Rev. Lett. **62** 1564
- [145] Lüscher A, Milstein A I and Sushkov 2007 Phys. Rev. Lett. **98** 037001
- [146] Sanna S, Allodi G, Concas G and De Renzi R 2005 *J. Supercond.* **18** 769
- [147] Stock C *et al.* 2006 Phys. Rev. B **73** 100504(R)
- [148] Curro N J, Milling C, Haase J and Slichter C P 2000 Phys. Rev. B **62** 3473
- [149] Mitrović V F *et al.* 2001 *Nature* **413** 501
- [150] Mitrović V F *et al.* 2003 Phys. Rev. B **67** 220503(R)
- [151] Kakuyanagi K, Kumagai K and Matsuda Y 2002 Phys. Rev. B **65** 060503
- [152] Kakuyanagi K, Kumagai K, Matsuda Y and Hasegawa M 2003 Phys. Rev. Lett. **90** 197003
- [153] Lake B *et al.* 2001 *Science* **291** 1759
- [154] Kadono R *et al.* 2004 Phys. Rev. B **69** 104523
- [155] Lake B *et al.* 2002 *Nature* **415** 299
- [156] Katano S, Sato M, Yamada K, Suzuki T and Fukase T 2000 Phys. Rev. B **62** 14677(R)
- [157] Khaykovich B *et al.* 2005 Phys. Rev. B **71** 220508(R)
- [158] Sonier J E *et al.* 2007 Phys. Rev. B **76** 064522
- [159] Lee S L *et al.* 1993 Phys. Rev. Lett. **71** 3862
- [160] Lake B *et al.* 2005 *Nature Materials* **4** 658
- [161] Savici A T *et al.* 2005 Phys. Rev. Lett. **95** 157001
- [162] Machtoub L H, Keimer B and Yamada K 2005 Phys. Rev. Lett. **94** 107009
- [163] Miller R I *et al.* 2002 Phys. Rev. Lett. **88** 137002
- [164] Sonier J E *et al.* 2003 Phys. Rev. Lett. **91** 147002
- [165] Sonier J E *et al.* 2004 *Physica C* **408** 783
- [166] Kadono R *et al.* 2004 J. Phys. Soc. Jpn. **73** 2944
- [167] Kadono R *et al.* 2005 J. Phys. Soc. Jpn. **74** 2806
- [168] Fujita M, Matsuda M, Katano S and Yamada K 2004 Phys. Rev. Lett. **93** 147003
- [169] Kadono R *et al.* 2003 J. Phys. Soc. Jpn. **72** 2955
- [170] Kang H J *et al.* 2005 Phys. Rev. B **71** 214512
- [171] Demler E, Sachdev S and Zhang Y 2001 Phys. Rev. Lett. **87** 067202
- [172] Park T *et al.* 2006 *Nature* **440** 65
- [173] Kivelson S A, Lee D -H, Fradkin E and Oganesyan V 2002 Phys. Rev. B **66** 144516
- [174] Khaykovich B *et al.* 2002 Phys. Rev. B **66** 014528
- [175] Boebinger G S *et al.* 1996 Phys. Rev. Lett. **77** 5417
- [176] Fournier P *et al.* 1998 Phys. Rev. Lett. **81** 4720
- [177] Ono S *et al.* 2000 Phys. Rev. Lett. **85** 638
- [178] Li S Y *et al.* 2002 Phys. Rev. B **65** 224515
- [179] Dagan Y *et al.* 2004 Phys. Rev. Lett. **92** 167001
- [180] Dagan Y *et al.* 2005 Phys. Rev. Lett. **94** 057005
- [181] Sun X F, Komiya S, Takeya J and Ando Y 2003 Phys. Rev. Lett. **90** 117004
- [182] Hawthorn D G *et al.* 2003 Phys. Rev. Lett. **90** 197004
- [183] Sun X F, Segawa K and Ando Y 2004 Phys. Rev. Lett. **93** 107001
- [184] Marchetti P A, Su Z B and Yu L 2001 Phys. Rev. Lett. **86** 3831
- [185] Marchetti P A, De Leo L, Orso G, Su Z B and Yu L 2004 Phys. Rev. B **69** 024527
- [186] Tallon J L and Loram J W 2001 *Physica C* **349** 53
- [187] Panagopoulos C *et al.* 2004 Phys. Rev. B **69** 144510
- [188] Panagopoulos C and Dobrosavljević V 2005 Phys. Rev. B **72** 014536